REPORT DOCUMENTATION PAGE

Form Approved
OMB No 0704 0188

1a REPORT SECURITY CLASSIFICATION Unclassified	1b RESTRICTIVE MARKINGS
2a SECURITY CLASSIFICATION AUTHORITY	3 DISTRIBUTION / AVAILABILITY OF REPORT Approved for public release;
2b DECLASSIFICATION / DOWNGRADING SCHEDULE	distribution is Unlimited.
4 PERFORMING ORGANIZATION REPORT NUMBER(S)	5 MONITORING ORGANIZATION REPORT NUMBER(S)
6a NAME OF PERFORMING ORGANIZATION Naval Postgraduate School 6b OFFICE SYMBOL (If applicable) 35	7a NAME OF MONITORING ORGANIZATION Naval Postgraduate School
6c ADDRESS (City, State, and ZIP Code) Monterey, Ca 93943-5000	7b ADDRESS (City, State, and ZIP Code) Monterey, Ca 93943-5000
8a NAME OF FUNDING / SPONSORING ORGANIZATION 8b OFFICE SYMBOL (If applicable)	9 PROCUREMENT INSTRUMENT IDENTIFICATION NUMBER
8c ADDRESS (City, State, and ZIP Code)	10 SOURCE OF FUNDING NUMBERS PROGRAM ELEMENT NO / PROJECT NO / TASK NO / WORK UNIT ACCESSION NO

11 TITLE (Include Security Classification)

AUTOMATED SATELLITE IMAGE NAVIGATION (UNCLASSIFIED)

12 PERSONAL AUTHOR(S)
Robert M. Bassett

13a TYPE OF REPORT	13b TIME COVERED	14 DATE OF REPORT (Year Month Day)	15 PAGE COUNT
Master's Thesis	FROM _____ TO _____	December 1992	89

16 SUPPLEMENTARY NOTATION The views expressed in this thesis are those of the author and do not reflect the official policy or position of the Department of Defense or the U.S. Government.

17 COSATI CODES			18 SUBJECT TERMS (Continue on reverse if necessary and identify by block number)
FIELD	GROUP	SUB-GROUP	image navigation, binary correlation, automated landmarking

19 ABSTRACT (Continue on reverse if necessary and identify by block number)

This study investigated the automated satellite image navigation method (Auto-Avian) developed and tested by Spaulding (1990) at the Naval Postgraduate School. The Auto-Avian method replaced the manual procedure of selecting Ground Control Points (GCP's) with an autocorrelation process that utilizes the World Vector Shoreline (WVS) provided by the Defense Mapping Agency (DMA) as a "string" of GCP's to rectify satellite images. The automatic cross-correlation of binary reference (WVS) and search (image) windows eliminated the subjective error associated with the manual selection of GCP's and produced accuracies comparable to the manual method.

This study expanded the scope of Spaulding's (1990) research. The worldwide application of the Auto-Avian method was demonstrated in three world regions (eastern North Pacific Ocean, eastern North Atlantic Ocean and Persian Gulf). Using five case studies, the performance of the Auto-Avian method on "less than optimum" images (i.e.,

20 DISTRIBUTION / AVAILABILITY OF ABSTRACT	21 ABSTRACT SECURITY CLASSIFICATION
☒ UNCLASSIFIED/UNLIMITED ☐ SAME AS RPT ☐ DTIC USERS	Unclassified
22a NAME OF RESPONSIBLE INDIVIDUAL Professor C. H. Wash	22b TELEPHONE (Include Area Code) (408) 656-2295 22c OFFICE SYMBOL MR/WX

DD Form 1473, JUN 86 Previous editions are obsolete. SECURITY CLASSIFICATION OF THIS PAGE

S/N 0102-LF-014-6603

T260261

(block 19 cont.)
islands, coastlines affected by lateral distortion and/or cloud cover) was investigated.

The results indicated that utilizing the Auto-Avian method on these "less than optimum images" could achieve navigational accuracies approaching those obtained by Spaulding (1990).

Approved for public release; distribution is unlimited.

Automated Satellite Image Navigation

by

Robert M. Bassett
Lieutenant Commander, United States Navy
B.S., University of Mississippi, 1980

Submitted in partial fulfillment
of the requirements for the degree of

MASTER OF SCIENCE IN METEOROLOGY AND PHYSICAL OCEANOGRAPHY

from the

NAVAL POSTGRADUATE SCHOOL
December 1992

ABSTRACT

This study investigated the automated satellite image navigation method (Auto-Avian) developed and tested by Spaulding (1990) at the Naval Postgraduate School. The Auto-Avian method replaced the manual procedure of selecting Ground Control Points (GCP's) with an autocorrelation process that utilizes the World Vector Shoreline (WVS) provided by the Defense Mapping Agency (DMA) as a "string" of GCP's to rectify satellite images. The automatic cross-correlation of binary reference (WVS) and search (image) windows eliminated the subjective error associated with the manual selection of GCP's and produced accuracies comparable to the manual method.

This study expanded the scope of Spaulding's (1990) research. The worldwide application of the Auto-Avian method was demonstrated in three world regions (eastern North Pacific Ocean, eastern North Atlantic Ocean and Persian Gulf). Using five case studies, the performance of the Auto-Avian method on "less than optimum" images (i.e., islands, coastlines affected by lateral distortion and/or cloud cover) was investigated. The results indicated that utilizing the Auto-Avian method on these "less than optimum images" could achieve navigational accuracies approaching those obtained by Spaulding (1990).

TABLE OF CONTENTS

I. Introduction 1

II. Background 5

A. Review of Image Navigation Techniques 5

B. Image Navigation Accuracies 8

C. AVHRR Navigation Adjustment (ANA) 9

1. Method Description 10

a. Data Preprocessing 10

b. Landmark File Generation 12

c. Cloudy Landmark Rejection 12

d. Reference Window Construction 14

e. Actual Window Construction 15

f. Navigation Error Calculation 16

g. Quality Control 17

h. Error Correction Application 19

2. Accuracy of the Method 19

D. Automated Image Navigation System 21

1. Method Description 22

a. Data Preprocessing 22

b. Shoreline File Generation 22

c. Image Sub-scene Selection 25

d. Binary AVHRR Sub-scene Construction . . 25

e. Binary Reference Sub-scene Construction 27
f. Window Selection 30
g. Navigation Error Calculation 32
h. Error Correction Application 33
2. Accuracy of the Method 35

III. METHODOLOGY 38
A. Motivation 38
B. Procedure 40
C. Case Studies 43
1. Case 1 44
2. Case 2 45
3. Case 3 45
4. Case 4 46
5. Case 5 47

IV. RESULTS 48
A. Case Study Highlights 48
1. Case 1 48
2. Case 2 50
3. Case 3 54
4. Case 4 56
5. Case 5 63

V. CONCLUSIONS AND RECOMMENDATIONS 68
A. CONCLUSIONS 68

B. RECOMMENDATIONS 69

1. Transition To The UNIX System 70

2. Increase The Level of Automation 70

3. Start Operational Use and Testing 70

LIST OF REFERENCES 72

INITIAL DISTRIBUTION 75

LIST OF FIGURES

Figure 1. ANA method flowchart with (R) and (A) representing the reference window and actual window respectively. Bordes et al. (1991) 11

Figure 2 Distribution of landmarks used for the ANA method (Bordes et al., 1991) 13

Figure 3 Illustration of landmark coordinate conversion process. Panel(a) Geographic coordinates, Panel(b) Satellite coordinates with rectangular reference window in solid lines (Bordes et al., 1991) 15

Figure 4. Illustration of navigation error resulting from similarity coefficient adjustment (Bordes et al., 1991) 18

Figure 5 Flowchart of the Auto-Avian method 23

Figure 6. WVS Ocean Basin Areas (DMA, 1988) 26

Figure 7 AVHRR subscene (Channel 2) 28

Figure 8 Corresponding Binary AVHRR Sub-scene 29

Figure 9 Mercator Projection of WVS 29

Figure 10 POS Projection of WVS 30

Figure 11 Binary reference and search images overlaid 31

Figure 12 Reference window centered inside search window (Spaulding, 1990) 31

Figure 13 WVS (White) and AVHRR sub-scene overlaid before Auto-Avian 34

Figure 14 WVS (White) and AVHRR sub-scene overlaid after Auto-Avian 34
Figure 15 WVS display before reduction (1:250,000 scale) 42
Figure 16 WVS display after reduction (1:500,000 scale) 42
Figure 17 Case 1 AVHRR Overview of NOAA-9 for 223430Z, 28 June, 1987 49
Figure 18 Case 2 AVHRR Overview of NOAA-11 for 233134Z, 10 May, 1992 51
Figure 19 Variability of pixel size with scan geometry (Bethke, 1988) 52
Figure 20 Surface resolution of HRPT imagery (NEPRF, 1983) 53
Figure 21 Navigation Error before Auto-Avian method: The WVS depicted in white. Subscene of Fig. 18. . . . 53
Figure 22 Navigation error after Auto-Avian method. The WVS depicted in white. Subscene of Fig 18 54
Figure 23 Case 3 AVHRR Overview of NOAA-9 for 225150Z, 17 June, 1987 55
Figure 24 WVS (white) offset after Auto-Avian method. Subscene of Fig. 23. 56
Figure 25 Case 4 AVHRR Overview of NOAA-11 for 155615Z, 8 June, 1992 57
Figure 26 Channel 2 image of Maderia, subscene of Fig 25. The Island is in the center of the image 58
Figure 27 Binary AVHRR (Channel 2) sub-scene (Fig. 26) 59

Figure 28 Ratio of albedos (Ch. 1/Ch. 2) image of Maderia. 60
Figure 29 Binary AVHRR (ratio of albedos) sub-scene. . 60
Figure 30 WVS (White) overlaid on image (Channel 2) of Maderia after Auto-Avian adjustment. 61
Figure 31 Residual error after Auto-Avian method . . . 63
Figure 32 Case 5 AVHRR Overview of NOAA-11 for 102623Z, 1 March, 1991 64
Figure 33 Coastal feature locations before Auto-Avian. (1) Single Island, (2) Simple Coastline and (3) Island-Coast Combination. 65
Figure 34 Coastal features after Auto-Avian. 66
Figure 35 Unsuccessful autocorrelation of island-coastline combination. 67

LIST OF TABLES

Table 1 CURRENT ACCURACIES OF AVHRR IMAGE NAVIGATION SCHEMES. 9

Table 2 NAVIGATION ERROR COMPARISON BETWEEN ANA METHOD AND MANUAL METHOD. (BORDES ET AL., 1991). 20

Table 3 ACCURACIES OF MANUAL AND AUTOMATED NAVIGATION METHODS (SPAULDING, 1990). 36

Table 4 ACCURACIES (KM) OF MANUAL AND AUTOMATED AVIAN METHODS. 50

ACKNOWLEDGEMENTS

Many thanks to Professor C. H. Wash and Professor P.A. Durkee for their patient guidance throughout the entire thesis process. A special thank you to Mike Thomas at the Defense Mapping Agency and Tom Wescott at the Naval Ocean Systems Center for providing much of the computer code and World Vector Shoreline data used in this research. Finally, I would like to thank Craig Motell, Kurt Nielsen and Chuck Skupniewicz for sharing their expertise in computer programming.

I. Introduction

It has been well-documented that the mapping of satellite images is affected by changes in the satellite's attitude and orbit. These effects can result in significant errors of 10-15 km when attempting to "earth locate" or assign a geographic position to an image pixel. While errors of this magnitude may have little impact on studies of synoptic scale meteorological and oceanographic events, more detailed studies of smaller scale events demand greater navigational accuracy. At the same time there is an increasing operational requirement to attain this greater accuracy via a method that is fast, reliable and requires a minimum of human intervention.

Previous studies have demonstrated that navigational accuracies approaching the spatial resolution of Advanced Very High Resolution Radiometer (AVHRR) images (1.1 km) can be achieved. This "optimal" navigation has been achieved by the utilization of Ground Control Points (GCP's) in conjunction with either a "circular orbit" method involving a simple, circular orbital model and predicted orbital parameters or an "ephemeris data" method utilizing an elliptical orbital model and more accurate, updated ephemeris data. Two recent studies of note have been conducted by (i) Bordes et al. (1991) at the Centre de Météorologie Spatiale (CMS) and (ii) Spaulding

(1990) at the Naval Postgraduate School (NPS). Both endeavors are of particular interest because they involved the automation of the image navigation process, thereby significantly reducing the amount of operator interaction normally required.

The CMS AVHRR Navigation Adjustment (ANA) procedure is summarized as follows:

1. A reference database consisting of binary images of pre-selected coastal landmarks is generated.
2. Binary subscenes containing each applicable landmark are constructed from an actual AVHRR image.
3. Correlation between the two binary images (reference and actual) determines the navigational error for each landmark as well as the total navigational error for the image.
4. Quality control checks determine validity/application of the navigation adjustment.

Concurrent with the ANA development, a similar correlation procedure was developed and tested on the NPS Image Navigation System (AVIAN). Highlights of Spaulding's research are as follows:

1. The Defense Mapping Agency's (DMA) World Vector Shoreline (WVS) is utilized as a reference binary database with worldwide coverage.
2. A binary image of any non-specific coastline in a satellite subscene is constructed (search).
3. Comparison of operator selected windows within the two binary images (WVS and search) determines line shift and timing error.

4. Correlation results are utilized to calculate the optimum satellite attitude angles and timing correction to renavigate the satellite image.

The preceding discussion was intended to provide a brief overview of recent developments in automating the image navigation procedure. A more detailed description and comparison of each method is provided later in this thesis.

The researchers at CMS and NPS have demonstrated the feasibility of reducing human interaction in the image navigation process while still obtaining optimal navigational accuracies. Both studies, however, appear to be constrained to specific geographic areas and/or image quality. For example, Spaulding's research was limited to satellite images of the eastern North Pacific Ocean and cloud free coastline located near the center of the image.

The goal of this thesis is to expand the scope of Spaulding's automated image navigation procedure as follows:

1. Demonstrate and test the worldwide application of the procedure by providing the capability to extract, reduce and display WVS from diskette storage.

2. Investigate the accuracy of utilizing the procedure for "less than optimum" images, such as coastlines located on the lateral extremes of the image, coastlines masked by cloud cover and complicated by nearby islands.

3. Investigate cloud reduction techniques to better define the land - water interface of the image.

A more detailed discussion of recent image navigation procedures including a description of the automated Avian procedure follows in Chapter II. The methodology for the

study is outlined in Chapter III. Chapter IV contains the results of the study followed by conclusions and recommendations in Chapter V.

II. Background

A. Review of Image Navigation Techniques

Since the late 1970's, numerous image navigation techniques have been utilized attempting to achieve "optimal" accuracies approaching that of the sensor's instantaneous field of view (IFOV). These techniques are primarily based on either the "circular orbit" or the "ephemeris data" method of image navigation as described in the introduction. While the circular orbit approach can be accomplished in real-time and without updated ephemeris data (Ho and Aspen, 1986); the ephemeris data approach is more accurate (Emery et al, 1989). Past research indicates that both methods require Ground control Points (GCP's) to achieve the optimal accuracy (1.1 km) of AVHRR imagery (Emery and Ikeda, 1984).

The use of GCP's or landmarks in the registration of satellite imagery is well-documented. Goshtasby et al. (1986) described the registration process to correct for translational, rotational and scaling errors. For circular orbital models, these GCP's have been utilized to correct for numerous error sources including, but not limited to, the satellite orbit, satellite attitude, inclination angle, sensor scan geometry and variations in the shape of the Earth (Emery and Ikeda, 1984; Ho and Asem, 1986). While landmark

adjustments for elliptical models using updated ephemeris data primarily involve along track corrections due to such sources as atmospheric drag, solar wind and timing errors between the satellite and the tracking station. This meridional correction and/or "nudge" has been successfully applied by many researchers (Emery and Ikeda, 1984; Brush, 1988). The number of GCP's required to optimally navigate an image is dependent upon the basic method used for image navigation. Studies have shown that similar accuracies can be achieved with the circular method requiring seven GCP's as compared to the ephemeris data method requiring only one GCP (Emery and Ikeda, 1984). Consequently, in most cases the circular orbit method requires a larger landmark database, more operator intervention and is subject to a larger degree of human error. Due to these drawbacks, the ephemeris data method, while more complex, is generally the preferred image navigation scheme. None the less, research continues on procedures to automate the registration process, thereby reducing manual interaction and its associated errors.

Another method of image registration involves the use of correlation techniques and appears to be more easily adaptable for automation. Past studies have indicated that sub-scenes from two images can be cross-correlated using a similarity detection algorithm from which local shift parameters can be determined and applied to rectify the two images (Crombie, 1983; Henderson et al., 1985; Anuta and McGillem, 1986). Some

researchers have utilized binary gradient images in this cross-correlation process (Jayroe et al., 1974; Cordan and Patz, 1979). Typically a threshold value is applied to the gradient image thereby producing a binary image containing only two grey level values (i.e., minimum and maximum). The successful registration of binary gradient images utilizing edge correlation is outlined by Anuta and McGillem (1986). Binary image cross-correlation techniques can usually be simplified by identifying an edge at a boundary between two areas of different grey levels. For example, the land - water interface normally provides a distinctive edge. In this case a binary image would assign the water a grey level value of zero, while land and/or clouds would be assigned a value of 255. Gradient operators such as those discussed by Moik (1980) can be utilized to further enhance the edge. Correlation techniques using edge matching has been investigated by Nack (1977) as well as Wong and Hall (1979). Recent efforts to cross-correlate a distinct coastline in an image with a shoreline database of precise latitude/longitude coordinates effectively produces a "string of GCP's" for image registration (Bordes et al., 1991; Spaulding, 1990).

In order to simplify the cross-correlation process a method known as "template matching" is commonly used. Numerous researchers (Hall, 1979; Moik, 1980; Eversole and Nasburg, 1983; Goshtaby et al., 1984) have examined this method of locating a subset or window of a reference image

(template) within the bounds of a larger search image. In this routine the degree of similarity between the two images is calculated as the template is shifted to different positions within the search area. The shift position which produces the largest degree of similarity is then used to register the entire image. The similarity between the two images can be determined using either a cross-correlation coefficient (Moik, 1980; Hord, 1982; Goshtasby et al., 1984) or the sum of absolute differences (Vanderburg and Rosenfeld, 1977; Hord, 1982). Bordes et al. (1991) utilized the more accurate cross-correlation coefficient while Spaulding (1990) maximized computational efficiency by using the sum of absolute differences. A further discussion of each method is provided later in this chapter.

B. Image Navigation Accuracies

As previously outlined, there are several considerations in the determination of any particular navigation technique. Choices of orbital models, registration processes and degree of automation all influence the ultimate accuracy of the procedure. The preceding discussion has attempted to focus attention on recent efforts to achieve optimal navigation accuracy. Table 1 summarizes the current accuracies of various AVHRR image navigation schemes. The most recent

research conducted by Bordes et al. (1991) as well as Spaulding (1990) will be examined in greater detail.

TABLE 1. CURRENT ACCURACIES OF AVHRR IMAGE NAVIGATION SCHEMES

Author	Method	Accuracy (in Km)
Emery and Ikeda 1984	Circular Orbit, 7 GCP's	> 1.5
Ho and Asem 1986	Circular Orbit, 1 GCP	3
Brush 1988	Ephemeris Data, nudge	2 to 3
Emery and Ikeda 1984	Ephemeris Data, 1 GCP	> 1.5
Bethke 1988	Ephemeris Data, 2-16 GCP's	2 to 5
Kloster 1989	Ephemeris Data, 1 GCP, Grid	1 to 2
Spaulding 1990	Ephemeris Data, GCP String	1 to 1.7
Bordes et al. 1991	Ephemeris Data, GCP String	1.2 to 1.9

Note that Bordes et al. (1991) stated accuracy given in pixels and lines was converted to the approximate distance in km. at the nadir resolution (1.1 km).

C. AVHRR Navigation Adjustment (ANA)

The ANA method, in operational use at the Centre de Météorologie Spatiale (CMS), is one of the more recent attempts to automate image navigation. Bordes et al. (1991) fully described the development of this procedure. Basically, the method calculates navigation error via automatic correlation between windows of the actual image and pre-

selected coastal landmarks. The approach is similar to the one developed by Jullien and Phulpin (1988) and was adapted for use with the "ephemeris data" navigational model at the CMS (Brunel and Marsouin, 1987). The ANA method can be utilized for visual, near-infrared and infrared images and has produced navigation accuracies close to the full spatial resolution of the AVHRR (1.1 km). Figure 1 provides a flowchart of the ANA method described in this section.

1. Method Description

a. Data Preprocessing

Satellite data from the Advanced Very High-Resolution Radiometer (AVHRR) and the High Resolution Infrared Radiation Sounder (HIRS) are ingested and prepared for processing. Part of this processing includes an automatic cloud detection algorithm known as "LUX". This algorithm applies a series of threshold tests to various channel combinations in order to discriminate between cloudy and clear pixels. The daytime algorithm utilizes albedos (channels 1 and 2) and brightness temperatures (channels 4 and 5) to test for gross cloud cover, spatial coherence, dynamic visibility, channel 2/Channel 1 and thin cirrus (Saunders and Kriebel, 1988). A separate night-time algorithm was developed by Saunders and Kriebel, (1988) to test for gross cloud cover, spatial coherence, low, medium and high clouds using only the brightness temperatures from channels 3, 4 and 5. As a result

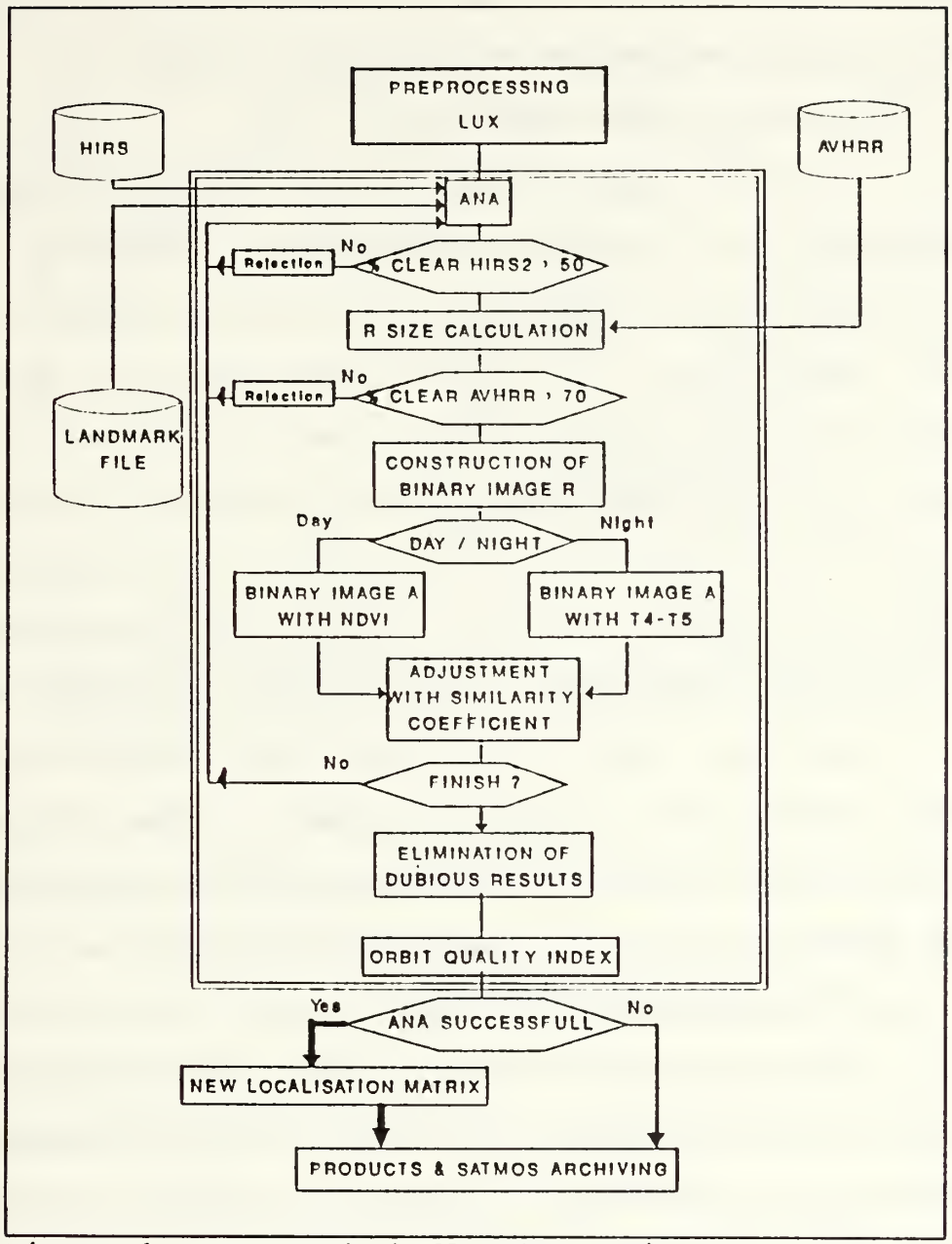

Figure 1 ANA method flowchart with (R) and (A) representing the reference window and actual window respectively. Bordes et al. (1991)

of these tests, the LUX process provides two key parameters ofimage cloudiness that are utilized later in the ANA method to reject landmarks obscured by clouds.

b. Landmark File Generation

A file of approximately 100, pre-selected landmarks was generated as a reference database. Landmarks were selected along the coast based upon their unique shape (i.e., islands, capes, bays, etc.). An atlas from the Service Hydrographique and Oceanographique de la Marine (SHOM) provided the source latitude/longitude points of the world's shoreline. Bordes et al. (1991) stated that the accuracy of the atlas was approximately 200 m. Each individual landmark record contains information such as name, size, landmark center flagged as land or sea and total number/list of shoreline points by latitude/longitude. The reference landmarks used for the ANA process were distributed throughout the CMS area of interest as illustrated in Figure 2.

c. Cloudy Landmark Rejection

As previously mentioned, the LUX preprocessing provides two key parameters upon which to base acceptance/ rejection of a selected landmark. First, a HIRS2 pseudochannel is used to indicate the percentage of clear pixels contained in a box (34 pixels x 39 lines) centered on a test point. Four test points are selected around the predicted landmark position and the clear-sky percentage is

approximated via linear interpolation. This preprocessing increases operational efficiency by rejecting landmarks where there is less than 50% clear sky.

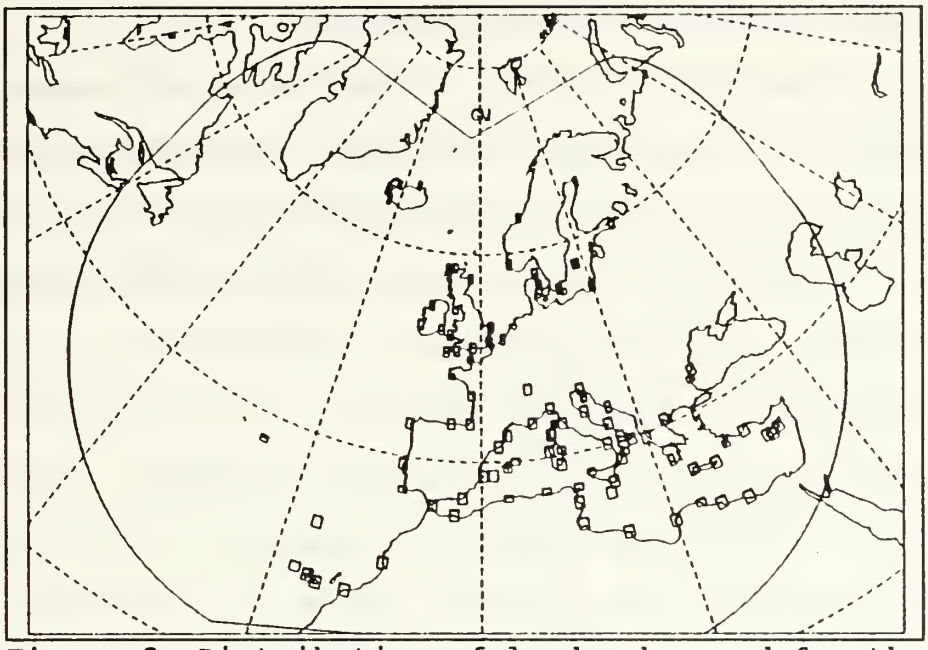

Figure 2 Distribution of landmarks used for the ANA method (Bordes et al., 1991)

If a selected landmark passes the first test, then the size of the reference window containing the landmark is calculated as described later in this thesis. At this point in the process a second cloudiness parameter is utilized to determine landmark suitability. The data preprocessing also provides an indicator of clear or cloudy pixels from which a cloud mask for the full resolution image can be generated. The cloud mask is constructed for a window 10 pixels and 10 lines larger than the reference window to account for navigation errors in the predicted landmark position. The

landmark is rejected if the clear-sky percentage calculated using this AVHRR cloud mask is less than 70%.

d. Reference Window Construction

"Reference windows" of pre-selected landmarks are constructed for comparison with full resolution windows of satellite imagery containing the predicted position of each reference point. The landmarks are converted from geographic coordinates (i.e., latitude and longitude) to satellite coordinates (i.e., line and pixel) so that similar errors throughout the image can be more easily compared. After this conversion process, the largest rectangular area in lines and pixels containing the landmark center is defined as the reference window. The reference window's size is dependent upon the specific landmark selected and the satellite's orbital parameters. Therefore, the dimensions of the reference window varies and is calculated for each landmark area and satellite pass. Figure 3 illustrates this conversion process and the delineation of the reference window.

As previously mentioned, the exact specifications of the reference window are required so that the second cloudiness test can be performed on the AVHRR image to eliminate obscured landmarks. The final step constructs a binary image of the landmark area contained in the reference window. Land areas are assigned a value of 0 while sea areas are assigned a value

of 1 as determined by the landmark center flag (land or sea) in the original database.

e. Actual Window Construction

"Actual windows" of the AVHRR imagery are constructed for correlation with the reference windows previously generated. The actual window encompasses and is

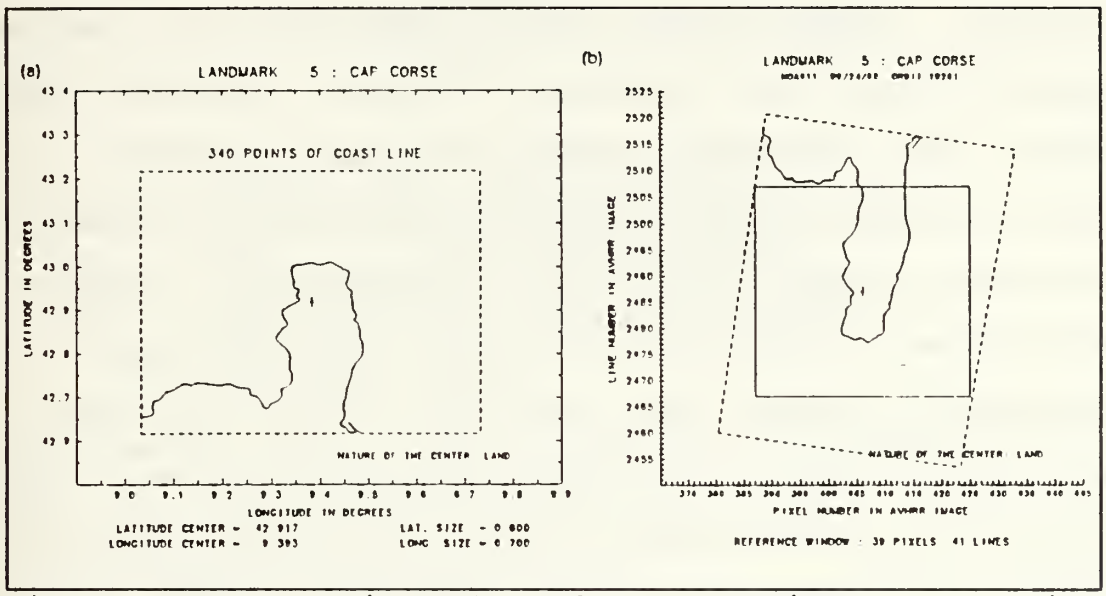

Figure 3 Illustration of landmark coordinate conversion process. Panel(a) Geographic coordinates, Panel(b) Satellite coordinates with rectangular reference window in solid lines (Bordes et al., 1991)

centered on the reference window. The size of the actual window is 16 pixels and 32 lines larger than the reference window to account for navigation error in predicting the landmark's position. Bordes et al. (1991) stated that the navigation error usually will not exceed ±8 pixels and ±16 lines based on their observations.

A binary image or "land-sea mask" is constructed of the actual window centered on the "cloud free" landmark (see cloudy landmark rejection procedures). There are two methods used to generate the land-sea mask depending upon the time of the image (i.e., Day or Night). For daytime images (channels 1 and 2), Bordes et al. (1991) determined the land-sea interface using the normalized difference vegetation index (NDVI). The procedure is fully described by Bordes et al. (1991) including the NDVI threshold utilized in the process. The second method utilizes the difference in brightness temperatures of the infrared channels (channels 4 and 5) to discriminate between land and sea. This procedure is particularly useful for nighttime images although some landmarks are rejected when a distinct difference between the land and sea temperatures is not observable. Bordes et al. (1991) outline the threshold adjustments necessary to generate the land-sea mask.

f. Navigation Error Calculation

The navigation error is calculated by comparing the two binary images (i.e., reference and actual) of a selected landmark area. This comparison process utilizes a "template matching" technique similar to the one described earlier in this chapter. In the ANA method, however, the reference window is cross-correlated with a "moving window" of the same dimensions that is shifted throughout the actual window. The

degree of similarity between the moving window and the reference window is computed via a similarity coefficient. Bordes et al. (1991) define this coefficient by the following equation:

$$S(i,j) = 1 - \left(\sum_{p=1}^{NP_r} \sum_{l=1}^{NL_r} |A_{p+i,l+j} - R_{p,l}| \right) / NP_r NL_r \qquad (1)$$

A: binary matrix (actual window)
R: binary matrix (reference window)
NPa: number of pixels (actual window)
NLa: number of lines (actual window)
NPr: number of pixels (reference window)
NLr: number of pixels (reference window)
i: line displacement
j: pixel displacement

If the moving window perfectly matches the reference window, then S achieves a maximum value of 1. In practice, the optimum line and pixel displacement (i_{opt}, j_{opt}) which maximizes the value of S is used to compute the navigation error for a given landmark. Basically, the line and pixel shift represents the navigation error between the observed landmark center (o) in the cross-correlated moving window and the estimated landmark center (c) in the actual window. Figure 4 illustrates this navigation error. The details of the computation are outlined by Bordes et al. (1991).

g. Quality Control

Several quality control checks are conducted to validate the navigation adjustment. This validation is necessary because the actual landmarks may not be completely

cloud-free despite the use of cloud detection algorithms. Consequently, the presence of clouds may affect the calculation of the similarity coefficient and in turn the navigation adjustment. Therefore, checks are performed on individual landmarks as well as the entire set of landmarks

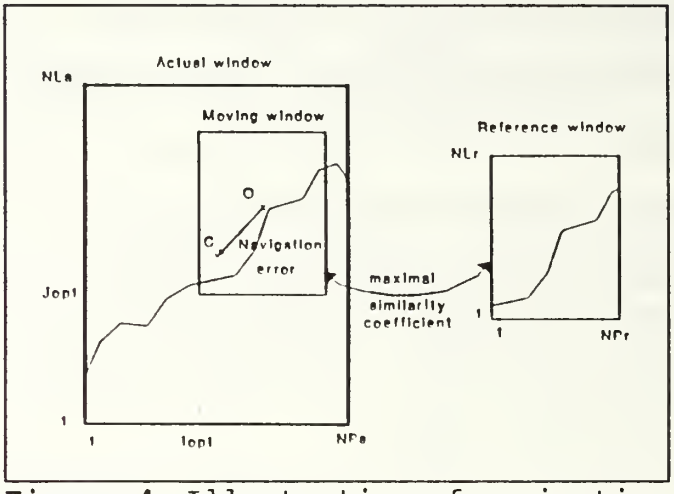

Figure 4 Illustration of navigation error resulting from similarity coefficient adjustment (Bordes et al., 1991)

available for a given pass. Individual landmarks are tested and rejected when 1) there is an insufficient amount of coastline and/or 2) the value of the similarity coefficient indicates an inadequate match (i.e., $S \leq 0.90$). The landmark set is also tested to ensure that 1) individual landmark error is consistent with the errors from other landmarks distributed throughout the image and 2) there is a sufficient number of valid landmarks for the entire image (i.e., Day > 3, Night > 4). Bordes et al. (1991) delineates the thresholds used in these tests.

h. Error Correction Application

The overall error correction for the entire image is obtained by averaging the individual navigation errors of the valid landmarks. This correction (line and pixel) is converted back to geographic coordinates (latitude and longitude) in determining the appropriate navigation adjustment for image registration. Prior to the application of this adjustment, however, the quality of the orbit is determined. Based on this determination, the navigation adjustment can be applied to 1) the current orbit, 2) the preceding orbit or 3) neither orbit. Once validated, the navigation adjustment is utilized to renavigate the image and subsequent satellite products.

2. Accuracy of the Method

Two images (day and night) were manually navigated utilizing an interactive console to visually control the image navigation (i.e., superimposing a coastline on the images). Using the console, Bordes et al. (1991) obtained the pixel and line numbers of visible landmarks in each image. From the day image (channel 2) with relatively clear coastlines 42 landmarks were selected while a smaller number (22) were selected from the night image (channel 4) due to cloud cover (Bordes et al., 1991). A separate database of landmark points (latitude and longitude) was used as a reference to calculate the "true" pixel and line numbers of the selected landmarks.

The pixel and line errors for each landmark were computed by subtracting the image values from the true values. The errors (pixel and line) of the manual navigation method were compared to these obtained using the ANA method. Table 2 provides the results of the comparison. Bordes et al. (1991) observed a good correlation between the two methods with any differences well within the standard deviation of the manual procedure. Based on this validation, the ANA process was placed in operational service in May, 1990.

TABLE 2. NAVIGATION ERROR COMPARISON BETWEEN ANA METHOD AND MANUAL METHOD. (BORDES ET AL., 1991)

	Pixel error		Line error		
Method	Mean	Sigma	Mean	Sigma	Number of landmarks
Orbit 7321 (day) on 25 February 1990					
ANA	3.68	0.55	-3.82	0.39	22 (24)
Manual	3.40	0.81	-3.99	1.01	42
Orbit 8005 (night) on 14 April 1990					
ANA	3.55	0.50	-0.91	1.08	11 (33)
Manual	4.11	1.01	-0.45	1.00	26

Over a seven month period (May - November, 1990), 86% of the total orbits (839) were successfully corrected using the ANA method. Bordes et al. (1991) observed a somewhat constant pixel error (3.0 mean), but the line error was much more variable (3.8 rms error). Based on these observations, a standard pixel correction is applied to all orbits when the ANA method is unsuccessful. No standard line correction is

applied, however, as the specific source of the error has not been fully determined. The possible causes of the line error are discussed in Bordes et al. (1991) with the most probable cause being satellite clock error.

To determine the overall accuracy of the navigation adjustment Bordes et al. (1991) calculated the mean standard deviations of the pixel and line errors corrected by the ANA method. Bordes et al. (1991) estimated that the accuracies ranged from 0.8 pixel and 1.0 line (current orbit adjustment) to 1.0 pixel and 1.7 lines (preceding orbit adjustment). For comparison purposes, this author converted these pixel and line values to their approximate distance (km) using the AVHRR nadir resolution (1.1 km). After conversion the accuracies ranged from 1.2 to 1.9 km.

D. Automated Image Navigation System

Automated registration procedures similar to the ANA method were developed for the Image Navigation System (AVIAN) at the Naval Postgraduate School (NPS). Spaulding (1990) outlined the design and testing of the procedure referred to as "AUTO-AVIAN". In effect, Auto-Avian replaces the manual landmarking procedure with an automated cross-correlation process for image registration. The technique involves the use of "template matching" to compare a binary reference shoreline with a binary gradient image. Cross-correlation results are used to adjust the navigation of the original

image. Experimental testing of the Auto-Avian procedure on visual AVHRR images has revealed near optimal navigation accuracies. A flowchart of the Auto-Avian method desribed in this section is provided by Figure 5.

1. Method Description

a. Data Preprocessing

Avian uses a "glean" routine to process raw satellite data, usually stored on magnetic tape. Files containing ephemeris data, raw calibration data and image scan data are produced by this routine for further processing. A reduced resolution overview of the entire pass must be created before the subsequent production of full resolution sub-scenes. Any available AVHRR channel can be utilized to create the overview which presents a "first look" at the overall image.

b. Shoreline File Generation

The Auto-Avian procedure requires a file of reference shoreline for the cross-correlation process. The Defense Mapping Agency's (DMA) World Vector Shoreline (WVS) provided the source database. The WVS is an ideal reference source due to its worldwide areal coverage and high accuracy requirements. The absolute horizontal accuracy requirement is that 90% of all identifiable shoreline features be located within 500 meters circular error of their true geographic positions with respect to the World Geodetic System 84 (WGS

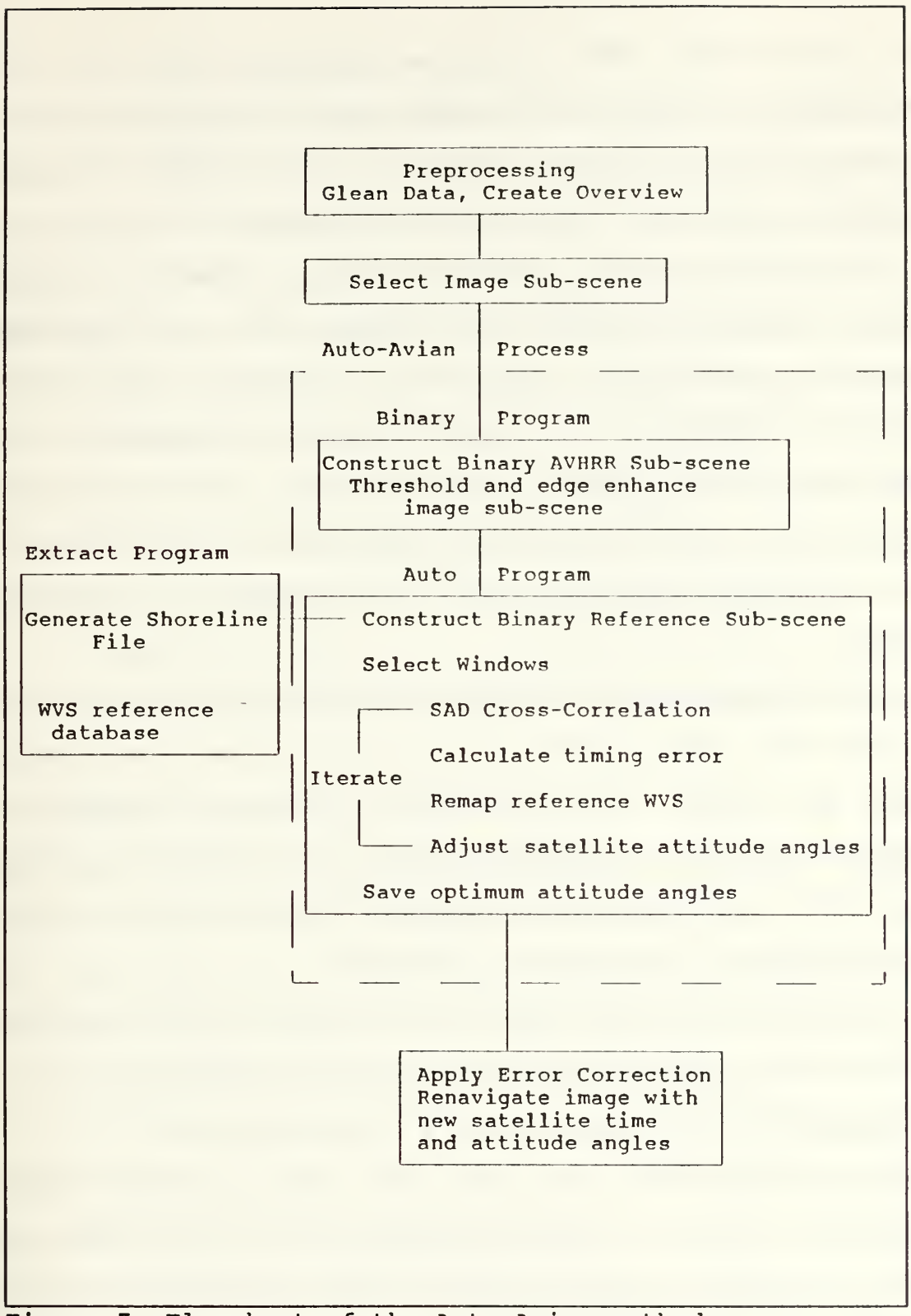

Figure 5 Flowchart of the Auto-Avian method

84) datum (DMA, 1988). It is important to note the compatibility between the WVS and satellite orbit datums which minimizes datum transformation error. This possible source of navigation error will be discussed in Chapter III.

The WVS is a digital database with an average of 12 data points (latitude/longitude) per nautical mile. The database consists of shorelines, international boundaries and country names as depicted on a 1:250,000 scale cartographic map. Spaulding (1990) reduced the resolution of the original database by selecting every 8th data point. The details of this reduction technique will be discussed in the next chapter.

To minimize redundant storage, the data structure utilizes a chain-node vector format as described by Spaulding (1990). None the less, the worldwide database encompasses approximately 160 megabytes. The data is commonly available on 9 track, 1/2 inch magnetic tape (6250 CPI) for the 10 ocean basin areas as illustrated in Figure 6.

A file of continuous shoreline included in the satellite coverage area must be extracted for the Auto-Avian procedure. The program used to ingest the WVS source data and select the reference coastline (i.e., U.S. West Coast) is explained by Spaulding (1990). The extracted file of latitude and longitude points is utilized later in the process to construct a binary reference sub-scene.

c. Image Sub-scene Selection

Using the image overview, the operator subjectively selects a sub-scene (512 x 512) of relatively cloud-free coastlines. The sub-scene is displayed utilizing a "paint" routine of the original Avian procedure as described by Spaulding (1990). As with the image overview, various channel combinations can be chosen. Spaulding (1990) observed that a ratio of albedos (channel 1/channel 2) reduced cloud effects and enhanced the land-sea boundary. Channel 2 images also produced a well defined coastline but did not reduce image cloudiness. An example of a representative sub-scene (channel 2) is shown in Figure 7. Further discussion of the enhancement techniques with examples are provided in Chapter III.

The selected sub-scene must contain a "window" of clear coastline which can be non-specific in location. Window choice and size will be covered later in this section. If the sub-scene meets this criteria then the image is stored and the starting line and pixel are recorded for further processing.

d. Binary AVHRR Sub-scene Construction

Construction of a binary image from the selected AVHRR sub-scene marks the beginning of the Auto-Avian procedure. The binary image is produced utilizing a program termed "Binary" to apply a grey level threshold to the gradient sub-scene. A threshold value (0-255) is subjectively

Figure 6 WVS Ocean Basin Areas (DMA, 1988)

chosen which maximizes the land - water contrast. For channel 2 images, Spaulding (1990) reported that a threshold value of 45 produced a sharp distinction between land and water. In this example, a binary image would assign water pixels (<45) a grey level value of zero and land/cloud pixels (≥45) a grey level value of 255.

A gradient operator is used to edge enhance the land - water interface contained in the binary image. To produce a binary sub-scene consisting only of shoreline, Spaulding (1990) chose the Robert's gradient operator as represented by the following equation:

$$R(i,j)=\sqrt{[(g(i,j)-g(i+1,j+1))^2+(g(i,j+1)-g(i+1,j))^2]} \quad (2)$$

where

R(i,j)	value of Robert's gradient operator at a cell or pixel
g(i,j)	a particular cell or pixel
i	line number (or row number)
j	pixel number or column number)

Figure 8 shows an example of a binary sub-scene created from a Channel 2 AVHRR image (Fig. 7). Additional examples of the binary sub-scenes created by this method and discussion of the procedure used in this study are presented later in the thesis.

e. Binary Reference Sub-scene Construction

A binary reference sub-scene corresponding to the binary AVHRR sub-scene (Fig. 8) is constructed utilizing a program known as "Auto". The Auto program performs all of the

required processes in the subsequent autocorrelation procedure. Auto's first step uses the starting line and pixel

Figure 7 AVHRR subscene (Channel 2)

of the AVHRR sub-scene (recorded earlier) to extract the reference coastline points bounded by the sub-scene. The extracted file of WVS points (latitude and longitude) are mapped into a satellite projection (line and pixel). The Polar Orbiter Satellite (POS) projection utilizes available ephemeris data for the conversion process. Figures 9 and 10 show how the WVS would appear in a mercator and POS projection respectively. In effect, a binary image of the reference shoreline (WVS) is produced which matches the satellite sub-scene's scale and projection.

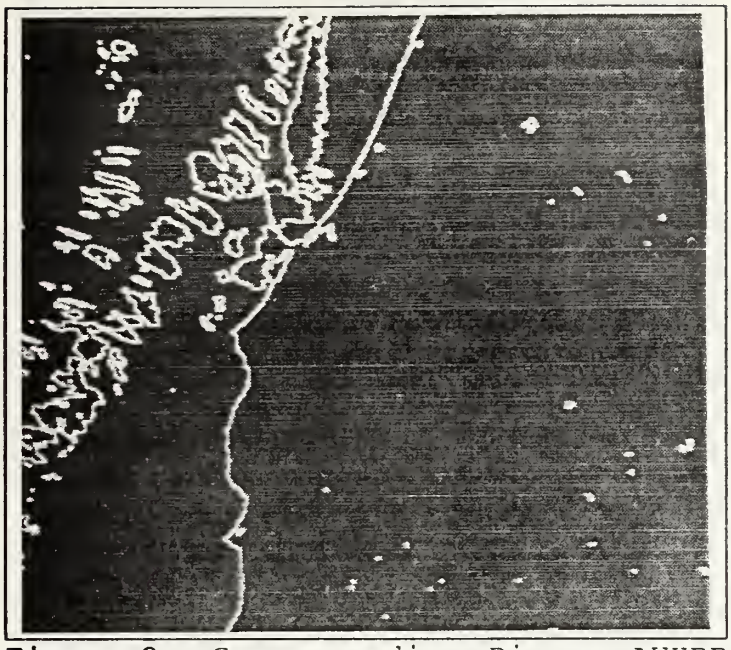

Figure 8 Corresponding Binary AVHRR Sub-scene

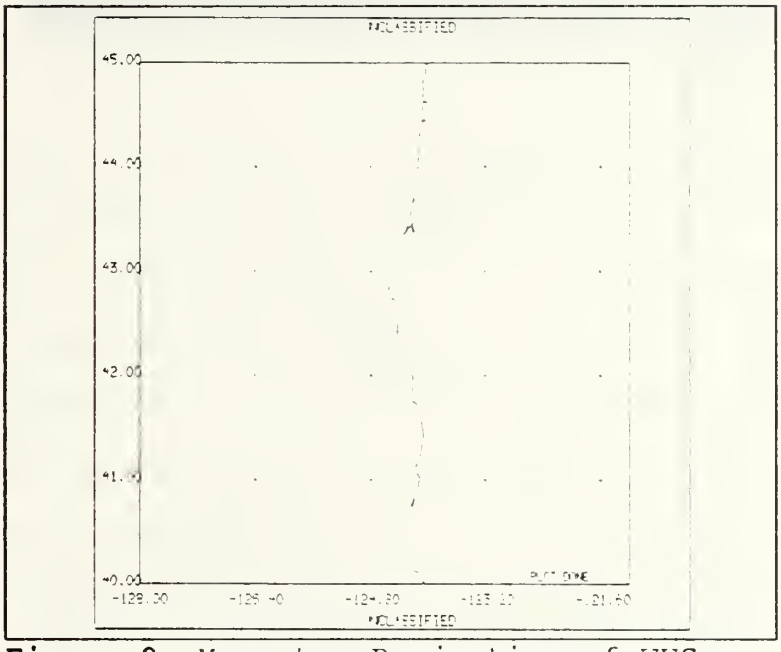

Figure 9 Mercator Projection of WVS

f. Window Selection

A "template matching" technique as previously described is used in the cross-correlation process. The Auto

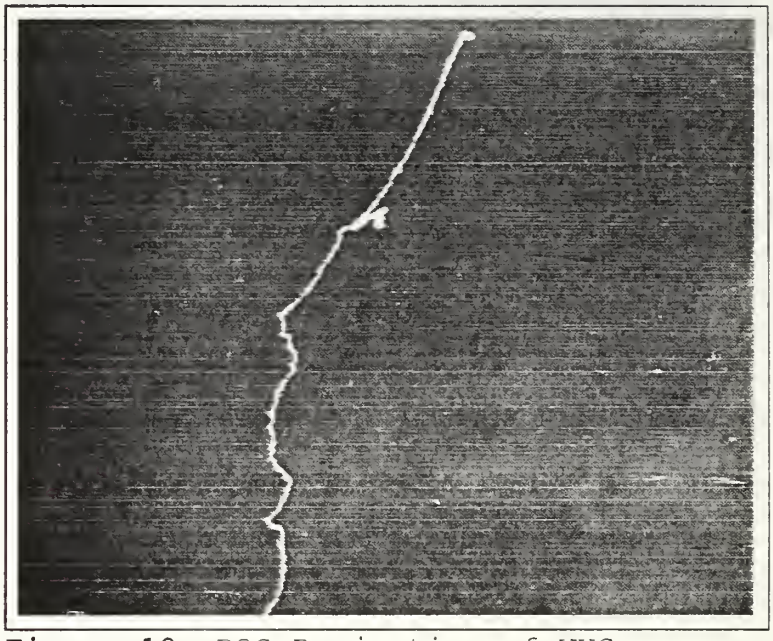

Figure 10 POS Projection of WVS

program displays the binary WVS sub-scene (reference image) overlaid on the binary AVHRR sub-scene (search image) for window selection (Fig. 11). The operator subjectively positions a cursor on a portion of distinct coastline contained in the reference image. Upon selection, the reference window is centered on the chosen point and enclosed within the search window as illustrated in Figure 12. The relative sizes of the windows are preset. The reference window is smaller (32 x 32 pixels) since it must be shifted throughout the search window (64 x 64 pixels) during the "matching" process. The dimensions of the windows were

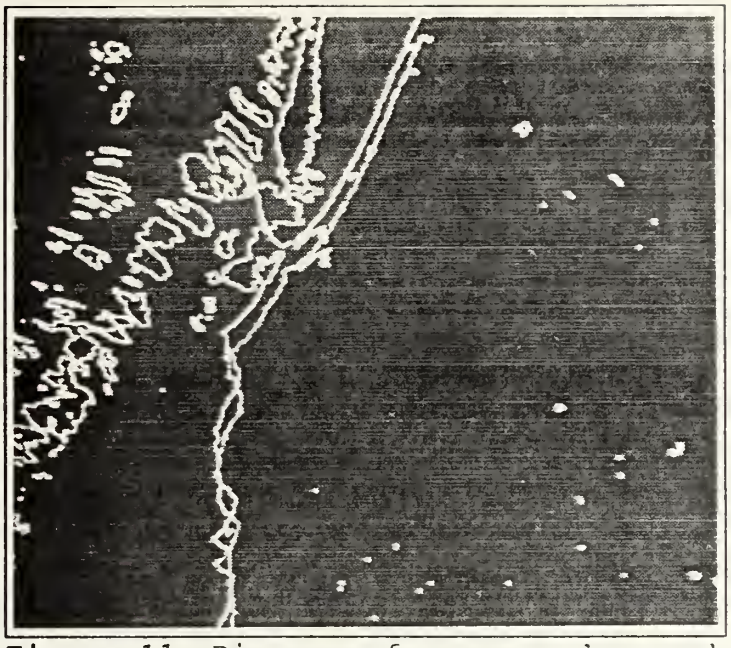

Figure 11 Binary reference and search images overlaid

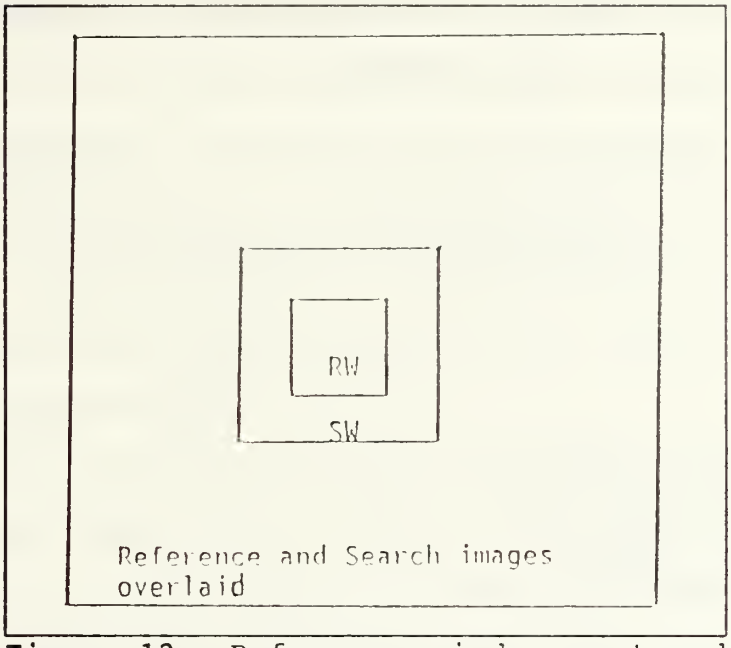

Figure 12 Reference window centered inside search window (Spaulding, 1990)

calculated such that the selected coastline would appear in both windows. Spaulding (1990) based the calculations upon the observed navigation error (12 km) from imagery navigated without landmarking procedures. The chosen window sizes accounts for the navigation error and theoretically insures a "match".

g. Navigation Error Calculation

The Auto program calculates the navigation error by cross-correlating the two binary shoreline images as the reference window is moved inside the search window. To measure the degree of similarity between the two windows, Spaulding (1990) used the sum of absolute differences (SAD) as defined by the following equation:

$$SAD=\sum\sum|s(i,j)-r(i+u,j+u)| \qquad (3)$$

s: search window
r: reference window
i: line number
j: pixel number
u: line and pixel shift

The SAD value is zero when the search and reference windows are a perfect match. The SAD values are calculated at numerous positions in the search window as described by Spaulding (1990). The shift position (line and pixel) which

results in the lowest SAD value (best match) is utilized to compute the along track timing error of the pass. Spaulding (1990) used the scan rate of the AVHRR radiometer (six lines per second) and the calculated line shift to correct for the timing error. Utilizing the corrected satellite time, the two windows are iteratively cross-correlated to determine the optimum satellite attitude angles. For each iteration the reference window's WVS is remapped into satellite coordinates and the satellite attitude angles are adjusted. The three angles (roll, pitch and yaw) each with three values (positive, negative and zero) results in 27 combinations of attitude angle adjustments. The attitude angles are adjusted in three increments of 5, 0.5 and 0.1 milliradians (Spaulding, 1990). For each adjustment increment, the attitude angles resulting in the smallest SAD value are used for the next increments' iteration. In the end, the Auto program provides the corrected satellite time and optimum attitude angles used to rectify the entire pass.

h. Error Correction Application

The time and attitude corrections are utilized to renavigate the AVHRR image. A "forward" routine of the original Avian procedure creates a new navigation file for the pass (Spaulding, 1990). Figures 13 and 14 shows the binary

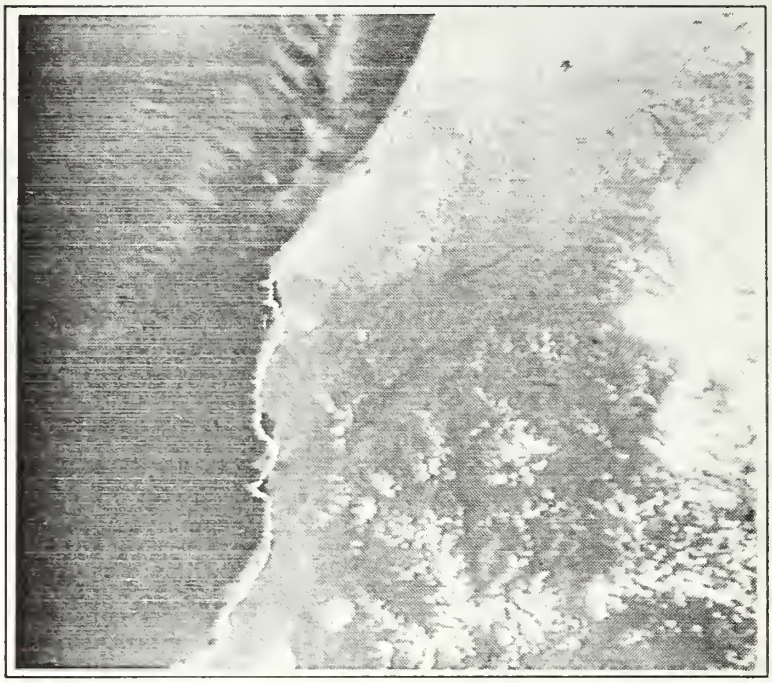

Figure 13 WVS (White) and AVHRR sub-scene overlaid before Auto-Avian

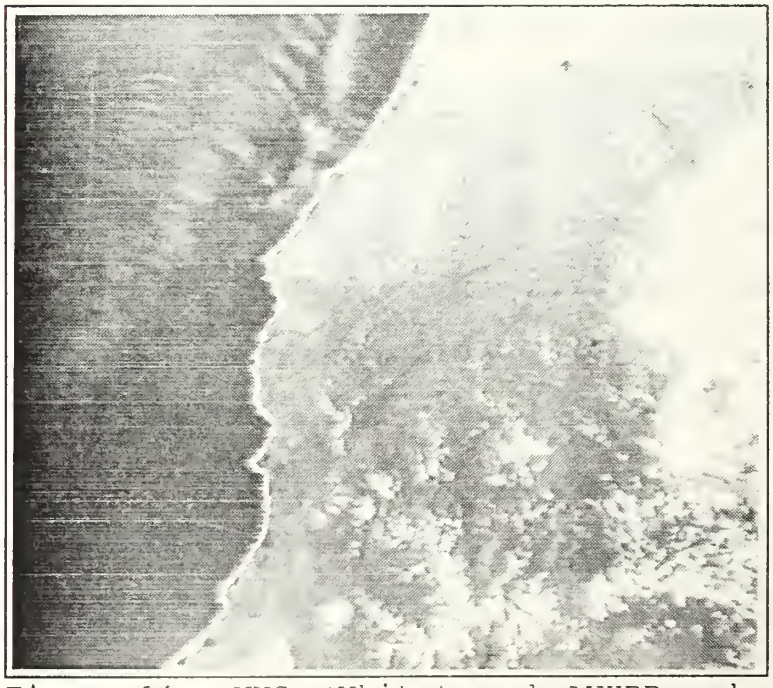

Figure 14 WVS (White) and AVHRR sub-scene overlaid after Auto-Avian

WVS sub-scene overlaid on the AVHRR subscene before and after the corrections are applied.

2. Accuracy of the Method

Ten AVHRR images of the Eastern North Pacific region were navigated with the original Avian procedure and the Auto-Avian method for comparison purposes. Each of the images contained some portion of relatively cloud-free coastline positioned close to and along the nadir of the pass. First, the original Avian procedure was used to navigate the images with no landmarks via the forward routine described by Spaulding (1990). The routine assumes the satellite's timing error and attitude angles are zero. Next, the images were renavigated utilizing Avian's manual landmarking procedures to subjectively select one and four GCP's. Finally, the image navigation was performed with the Auto-Avian method previously described in this section.

The accuracy of each navigation method was determined by utilizing the "known" locations of control points obtained from various cartographic sources. Spaulding (1990) stated that the control points were as evenly distributed over the image as possible and varied in number depending upon the quality of the image (control points obscured by clouds). The distance between the control point location (latitude and longitude) and the same point subjectively identified in the

image (converted to geographic coordinates) was calculated using the following equation from Bowditch (1984):

$$D=\cos^{-1}[(sinL_1 x sinL_2)+(cosL_1 x cosL_2 x cosDL_0)] \quad (4)$$

where

L1	Latitude of navigated point
L2	True latitude of the point
DL0	Difference between longitudes
D	Distance (in degrees)

To account for positioning and distortion errors in selecting individual control points, the average error distance was calculated from the set of control points contained in each image for each method of navigation (i.e., Auto-Avian, manual with zero, one and four GCP's). Since the number of control points varied among the ten images and the four navigation methods, Spaulding (1990) compared the results statistically by determining the mean and standard error of the mean for the set of images navigated by each method. Table 3 presents the accuracy results for the ten image set according to navigation method.

Table 3. ACCURACIES OF MANUAL AND AUTOMATED NAVIGATION METHODS (SPAULDING, 1990)

Statistic	0 Landmarks	1 Landmark	4 Landmarks	Auto Avian
Mean	12.32 km	1.92 km	1.46 km	1.32 km
S.E. of Mean	0.786 km	0.340 km	0.262 km	0.246 km

Utilizing the student's t statistic for unknown population variances, Spaulding (1990) determined with a 95% confidence

level that the Auto-Avian method was more accurate than the manual landmarking procedure with one GCP. Using the same criteria, Auto-Avian was not more accurate, however, than the manual landmarking procedure with four GCP's. Spaulding (1990) stated that although the manual procedure (four GCP's) and Auto-Avian method produced similar accuracies, the accuracy of the manual method is heavily dependent upon operator training and expertise. In comparison, the Auto-Avian method eliminated the subjective error associated with the manual selection of landmarks. The accuracies of the ten images navigated by the Auto-Avian method ranged from 1 to 1.69 km (Spaulding, 1990).

III. METHODOLOGY

A. Motivation

Three distinct differences between the ANA and Auto-Avian methods described in Chapter II provided the motivation for this study.

The first contrast concerns the capabilities of each method for image navigation on a worldwide basis. While the source database of the ANA method (SHOM atlas) delineates coastlines worldwide, the reference landmarks generated from this source are located primarily in the Western European region (Fig. 2). Bordes et al. (1991) did not specify the time required to generate the reference landmarks (100), but it could be inferred that utilizing the ANA method in other regions would require a reasonable amount of landmark preparation time. In contrast, the Auto-Avian method has the capability to extract any portion of the world's shoreline from the WVS digital database. Currently the shoreline points (latitude and longitude) contained in the area of operations must be extracted from the source database which is stored separately and readily available on magnetic tape according to ocean basin area (Fig. 6). Future improvements of the extraction process, data storage media and computer storage capabilities can ease access to the source data.

Although the extraction time is minimal, Spaulding (1990) did not test the Auto-Avian method outside of the eastern North Pacific Ocean region. Therefore, one of the goals of this study is to demonstrate and test the worldwide application of the Auto-Avian method.

A second area of interest concerns the orientation of reference landmarks or shoreline in relation to the satellite's ground track. For the ANA method, Bordes et al. (1991) stated that landmarks farther than 900 pixels from the nadir are eliminated by the HIRS2 cloudiness test. In comparison, the Auto-Avian method allows the operator to select any coastline, regardless of position, in the binary reference sub-scene. Despite this capability, the accuracy tests conducted by Spaulding (1990) only used coastlines positioned close to the ground track. This study will select reference coastlines located on the lateral extremes of the images to investigate the accuracy of the Auto-Avian method on "less than optimum" images.

Finally, the ANA and Auto-Avian methods utilize different techniques to process image landmarks or shorelines contaminated by clouds. The ANA method uses an automatic cloud detection algorithm (LUX) in conjunction with two tests of clear-sky fraction (HIRS and AVHRR) to objectively determine landmark suitability (Bordes et al., 1991). In the Auto-Avian method, however, image coastline selection is manual and highly subjective as described in the previous

chapter. This study will investigate the techniques utilized by Spaulding (1990) to reduce "cloud effects" with the prospect of automating the process in the future.

B. Procedure

The Auto-Avian method of image navigation developed by Spaulding (1990) was used as the basis for this study. The only change to the series of procedures delineated in Chapter II involved a modification of the shoreline file generation process. As previously stated, Spaulding (1990) extracted a file of reference shoreline points from the source WVS database stored on magnetic tape. The extraction program utilized by Spaulding (1990) reduced the resolution of the original WVS by selecting every 8th point and provided no capability to display the end product.

To improve the capabilities of the original extraction process, several computer routines were obtained from Defense Mapping Agency (DMA) and Naval Ocean Systems Center (NOSC) personnel. With minor modifications, these routines provided the capabilities to extract, reduce and display the WVS source data stored on computer diskette vice magnetic tape. Diskette storage furnished easier access to the source data which had been previously "thinned" (50m tolerance) to reduce the "stair-stepping" effect of the coastline (M. Thomas, personal communication). A modified polyline reduction routine (Douglas and Peuker, 1973) was used so that the reference

shoreline would approximately match the scale and accuracy of the satellite image (1:500,000). The routine utilizes a selected tolerance distance between points to reduce the scale of the data set (i.e., 250 m/1:500,000). Scale reduction using a tolerance distance tends to preserve coastline features that may be smoothed and/or eliminated by the arbitrary selection of data points (T. Wescott, personal communication). Figures 15 and 16 are displays of the WVS before and after reduction. Note the two displays are virtually identical.

A final routine provided the means to display and plot the extracted fine of shoreline used to construct the binary reference sub-scene. Some minor modifications to the "plot" routine allowed the operator to obtain precise positions (latitude and longitude) of specific coastline features. Approximately 67 precise positions were extracted from the WVS database to replace the corresponding GCP positions used in the manual landmarking procedure of the original Avian method.

There were two main reasons for replacing the original GCP locations. The first concern was to minimize the source errors of the landmarks. The original GCP positions were obtained from cartographic sources of various scales, accuracies and datums. The navigation error resulting from these sources could not be easily determined. For example, cartographic maps are frequently compiled on a local datum (i.e., North American 1927). Alone, the datum transformation

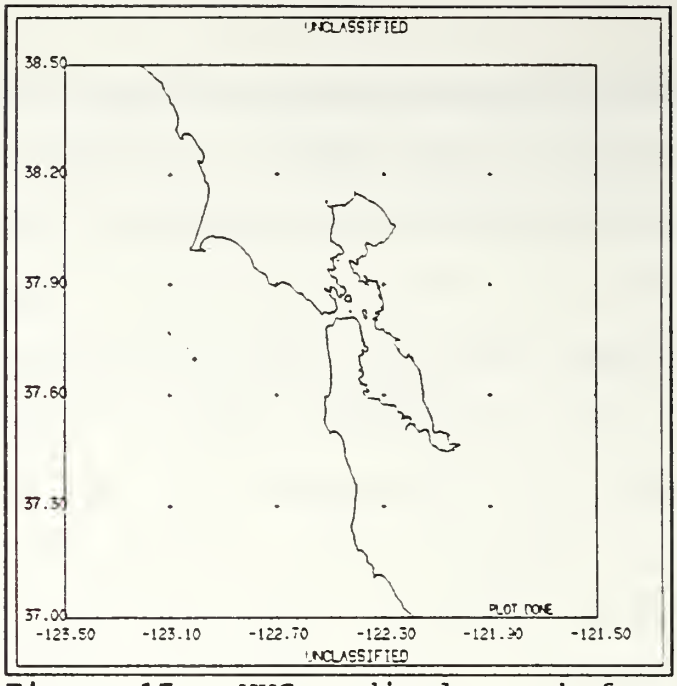

Figure 15 WVS display before reduction (1:250,000 scale)

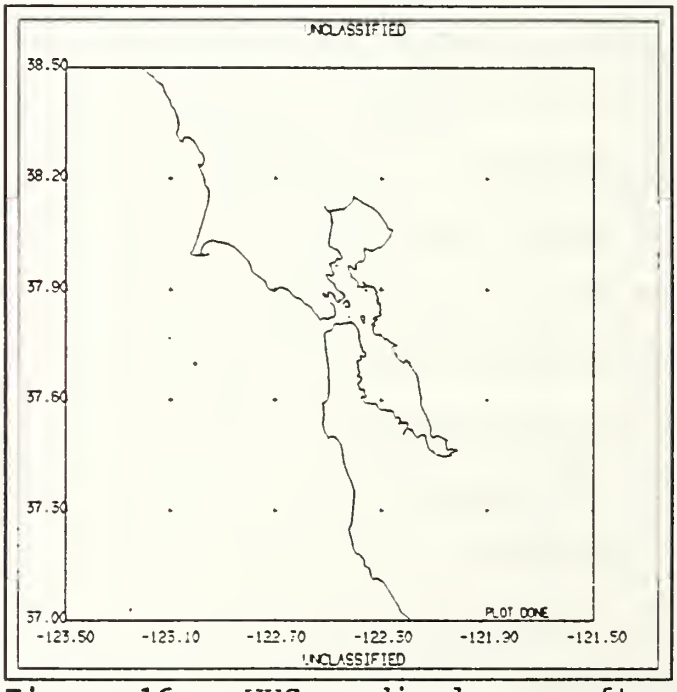

Figure 16 WVS display after reduction (1:500,000 scale)

error involved in comparing a map location (local datum) to a satellite location (WGS datum) could be hundreds of meters (DMA, 1990). The WVS GCP's (WGS 84) eliminated the datum transformation error and furnished a consistent "control" structure upon which to compare the manual and automated navigation methods.

The second concern was to minimize the subjective error associated with precisely locating the landmarks in an image. The subjective error is heavily dependent on the operator's level of training and expertise. Given a requisite level of expertise, having the same operator both select the GCP positions from a reference source and the actual image should reduce the amount of subjectivity. At worst, the errors would be consistent.

In effect, the single extraction routine used by Spaulding (1990) was replaced with three routines (i.e., extract, reduce and display) in this study. Although this change increased the time required to preprocess the WVS source data, the data manipulation capabilities were greatly enhanced allowing for a greater level of control. Future improvements of the Auto-Avian method could link together the separate routines to minimize data preprocessing time.

C. Case Studies

To expand the scope of the research conducted by Spaulding (1990), the cases used in this study spanned three world

regions, each with various orientations of the coastline and amounts of cloud cover. A total of five AVHRR images were navigated using the interactive landmarking procedures of the original Avian method (Spaulding, 1990) as well as the Auto-Avian method described in Chapter II. The residual navigation error after adjustment by each method (i.e., zero, one four GCP's and Auto-Avian) was determined utilizing a set of control points obtained from the WVS database and distributed evenly throughout each image. The calculated error distances (Bowditch, 1984) between the control point locations and the corresponding image locations were averaged to determine the overall accuracy of each method.

Selection of the five images used in this study was primarily based upon coverage region and coastline orientation. Overviews of each image are presented in the next chapter. The following is a narrative description of each case studied:

1. **Case 1**

The satellite area covered the eastern North Pacific Ocean region with the coastline of North America oriented along and near the ground track. The image was one of the ten images studied by Spaulding (1990) and served as a "control" case to ensure the Auto-Avian method was applied correctly in this study. Windows (reference and search) of the United States coastline were selected for cross-correlation. The

area selected (Cypress Point, CA) was affected by cloud cover; therefore, a ratio of albedos (Channel 1/Channel 2) was used to construct the AVHRR sub-scene. After the image was navigated with both manual and automated procedures, the residual navigation error was determined utilizing eight control points spaced at approximately equal distances along the coast.

2. Case 2

A second pass of the eastern North Pacific Ocean area was selected; however, in this case the shoreline was generally located farther than 900 pixels from the satellite's nadir. This "less than optimum" case was chosen to investigate the effect of lateral image distortion on the performance of the Auto-Avian method. A relatively short portion of cloud-free coastline was available for window placement. Due to the great amount of distortion, a clear and rather distinct feature (Point Reyes, CA) was selected for the autocorrelation process. The binary satellite sub-scene was produced by thresholding and edge enhancing a Channel 2 image. Only 6 control points were used to calculate the navigation error due to the limited availability of identifiable landmarks.

3. Case 3

To provide a better understanding of the relationship between window placement and accuracy of the automated method,

the areal coverage remained the same with the North American coastline extending from the nadir to the lateral extreme of the image. The Auto-Avian method was tested on three areas beginning near the center of the pass (Point Conception, CA) and subsequently moved towards the lateral edge (Angeles Island, MEX and Guaymas, MEX). Channel 2 was utilized to produce the binary AVHRR sub-scenes of the relatively cloud-free coastline. Landmark positions were easily identified throughout the image and compared with 11 control point locations to determine navigation accuracy.

4. Case 4

An image of the eastern North Atlantic Ocean region was selected to demonstrate the worldwide application of the Auto-Avian method. The coastline orientation was quite varied throughout the pass with the straits of Gibraltar located on the right lateral edge (>900 pixels), the island of Madeira approximately in the center and the Azores on the left lateral edge. Three window areas were chosen to test the autocorrelation procedure on an island (Madeira) and shoreline with varying degrees of lateral distortion (Cape Rhir, MOR and Cape Spartel, MOR). To reduce the effects of cloud cover around Madeira a ratio of albedos (Channel 1/Channel 2) sub-scene was generated while Channel 2 images were utilized for the could-free coastline of North Africa. The control points

(8) were distributed both horizontally and vertically throughout the image.

5. Case 5

The Persian Gulf region was chosen as the final case study. The region provided the opportunity to further investigate the capabilities of the Auto-Avian method. Several shoreline features from simple (single island) to complex (coastline near an island) were selected for testing. The vast majority of the landmass surrounding the Persian Gulf was free of cloud cover; therefore, Channel 2 sub-scenes provided distinct land-sea interfaces for cross-correlation. The control points (10) were located primarily along the perimeter of the Persian Gulf.

The five cases studied provided the means to test the Auto-Avian method under a wide variety of conditions. The navigation accuracy results of the automated method as compared to manual landmarking procedures are presented in the next chapter.

IV. RESULTS

The navigation results for the five case studies all presented in Table 4. Each AVHRR image was navigated by manual (zero, one and four landmarks) and automated (Auto-Avian) methods. For the manual method, the landmark point for the one GCP case was chosen near the center of the pass and in the four GCP case the points were distributed as evenly as possible throughout the pass. The calculated accuracies of the four methods varied considerably for each image depending upon the number and location (center, lateral edge, etc.) of control points. Similarly, the window placement (center, edge, island, etc.) for the Auto-Avian method also influenced the accuracy of the procedure. The effects of lateral distortion and pixel size on the accuracy values calculated for each method will be discussed later in this chapter. The following comments on each case study along with image overviews are intended to clarify the navigation accuracies obtained.

A. Case Study Highlights

1. Case 1

An image of the eastern North Pacific Ocean (Fig. 17) was chosen from the ten images utilized in the Spaulding (1990) study. The orbit's coverage area and coastline

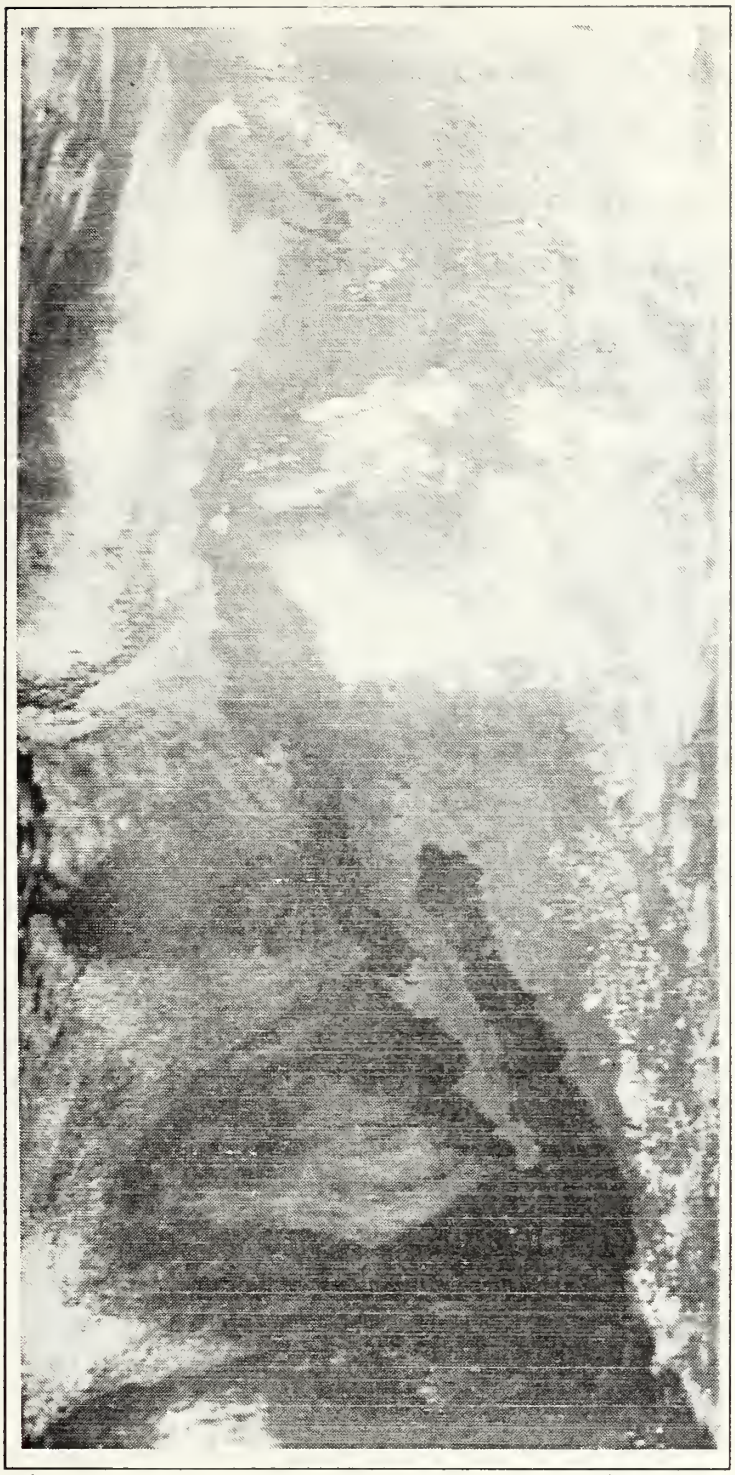

Figure 17 Case 1 AVHRR Overview of NOAA-9 for 223430Z, 28 June, 1987

orientation (near track) furnished a "typical" image as a control case for this research. The accuracies obtained from both manual and automated navigation methods compared well to those reported by Spaulding (1990). Based on these results, this researcher was reasonably assured of the proper operation and application of the experimental procedures.

TABLE 4. ACCURACIES (KM) OF MANUAL AND AUTOMATED AVIAN METHODS

Case	Tape Date	0 Landmarks	1 Landmark	4 Landmarks	Auto-Avian accuracy/ location
1	6-28-87	12.55	3.35	2.09	1.10/Mid-center
2	5-10-92	22.38	7.17	5.75	4.89/Far-Edge
3	6-17-87	14.48	2.86	1.87	1.84/Mid-Center
3	6-17-87	14.48	2.86	1.87	3.11/Mid-Edge
3	6-17-87	14.48	2.86	1.87	4.04/Far-edge
4	6-8-92	17.76	7.66	6.12	4.29/Center (Island)
4	6-8-92	17.76	7.66	6.12	9.55/Mid-edge
4	6-8-92	17.76	7.66	6.12	9.70/Far-edge
5	3-1-91	19.89	2.97	1.04	1.73/Center (Island)
5	3-1-91	19.89	2.97	1.04	4.12/Center
5	3-1-91	19.89	2.97	1.04	Unsuccessful/ Island-Coast

2. Case 2

Distortion effects on coastline located near the lateral extreme of the image (Fig. 18) was investigated in Case 2. The landmass was displaced to the far right of the satellite's track (>900 pixels) and oblique to the sensors'

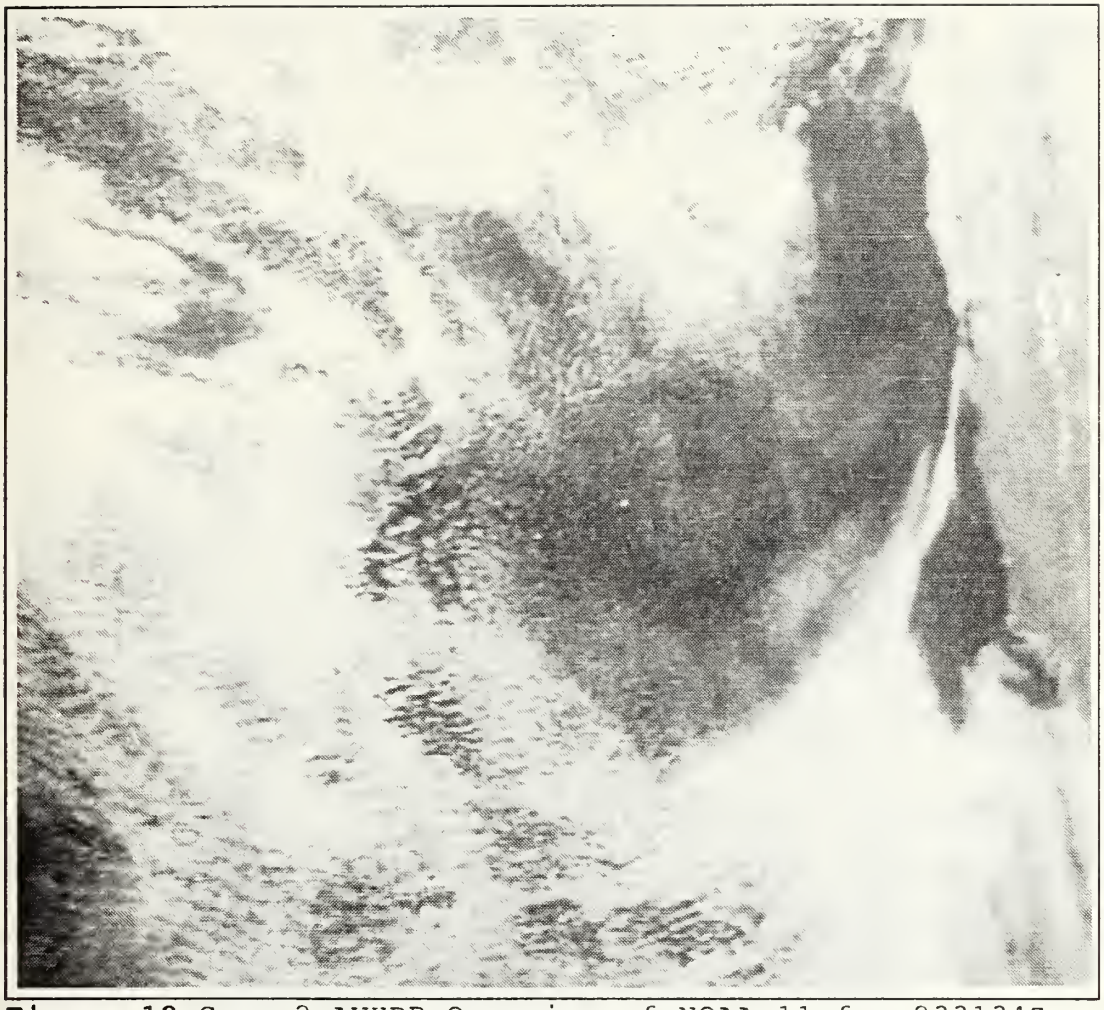

Figure 18 Case 2 AVHRR Overview of NOAA-11 for 233134Z, 10 May, 1992

line of sight (LOS). Bethke (1988) described the distortion resulting from this type of scan geometry and the variability of pixel size (Fig. 19). Using the approximate lateral displacement of the landmass (~750 n mi), the spatial resolution of the High Resolution Picture Transmission (HRPT) imagery was estimated to be 1.3 n mi (2.4 km) from Figure 20 (NEPRF, 1983). In view of the spatial resolution along the

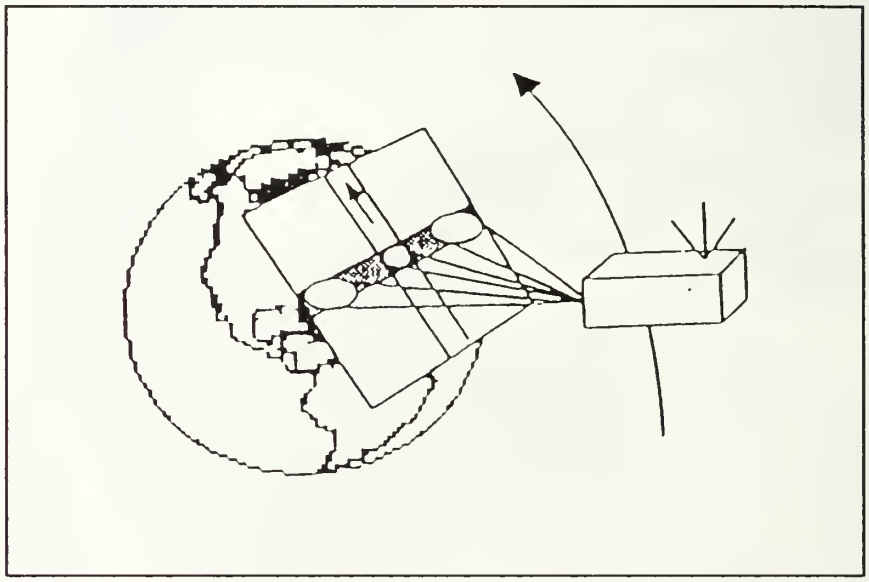

Figure 19 Variability of pixel size with scan geometry (Bethke, 1988)

coast, the Auto-Avian procedure navigated the "less than optimum" image to approximately two pixels (4.8 km). There was more residual navigation error, however, than the average one pixel error observed by Spaulding (1990). The additional error can be attributed to the increase in lateral distortion and its effect on the cross-correlation process. The results of the distortion on the matching process are evident in Figures 21 and 22.

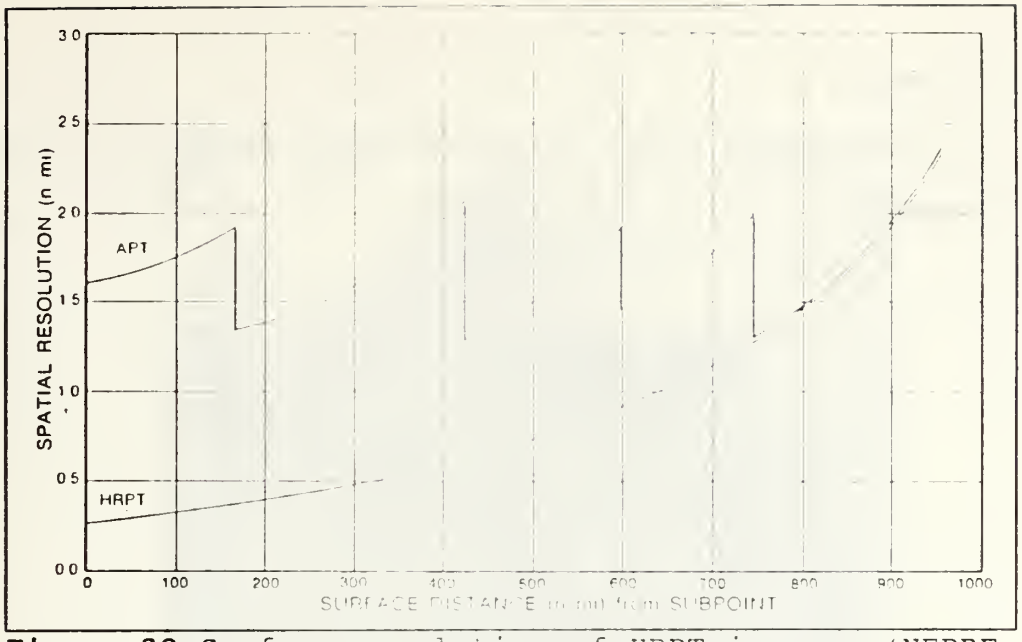

Figure 20 Surface resolution of HRPT imagery (NEPRF, 1983)

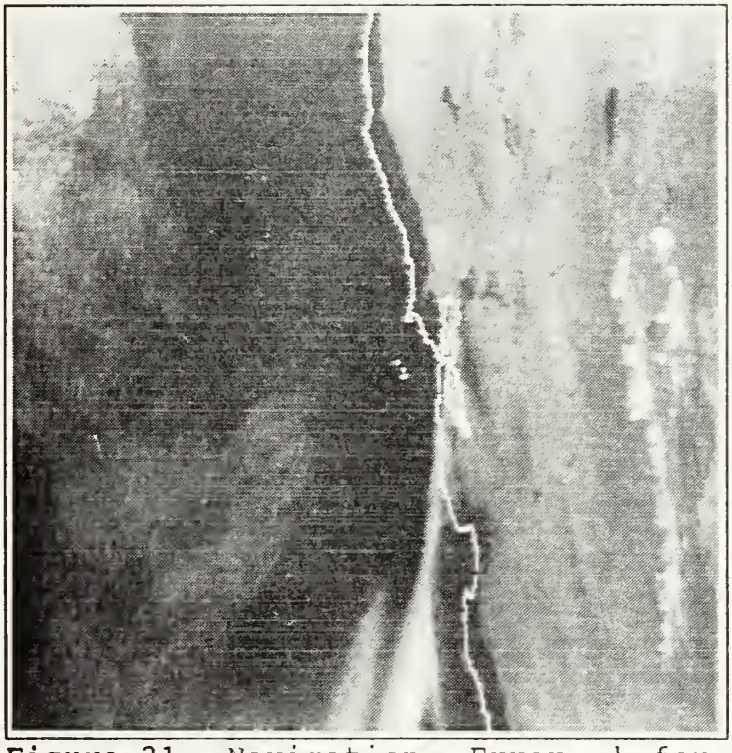

Figure 21 Navigation Error before Auto-Avian method: The WVS depicted in white. Subscene of Fig. 18.

3. Case 3

A third pass over the eastern North Pacific Ocean with the shoreline running from the center to the extreme right

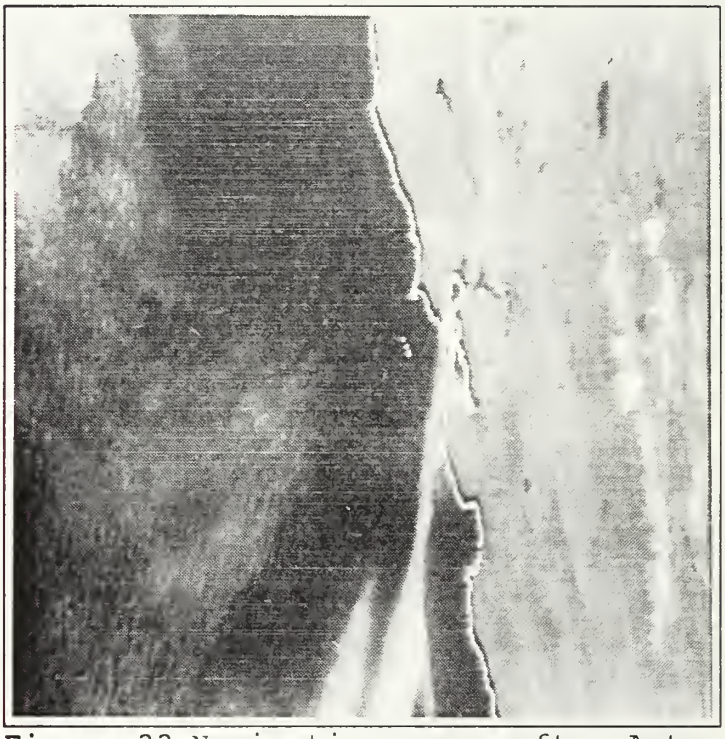

Figure 22 Navigation error after Auto-Avian method. The WVS depicted in white. Subscene of Fig 18

edge of the image (Fig. 23) was studied to further investigate the effects of distortion on the Auto-Avian process. For a window area selected near the center of the image (Point Conception, CA), the accuracy of the Auto-Avian process (1.84 km, Table 4) was comparable to the average accuracy (1.32 km) reported by Spaulding (1990). The accuracy of the method decreased as the window area was subsequently moved towards the right lateral edge. The resulting increase in distortion

Figure 23 Case 3 AVHRR Overview of NOAA-9 for 225150Z, 17 June, 1987

and pixel size caused an observable offset of the WVS. Figure 24 illustrates how the moderate distortion of a mid-edge window area (Angeles Island, MEX) can cause a slight offset of the reference shoreline. The residual error of the Auto-Avian method ranged from 3.11 km for the mid-edge window to 4.04 km for the far-edge window (Table 4).

Figure 24 WVS (white) offset after Auto-Avian method. Sub-scene of Fig. 23.

4. Case 4

The capability of the Auto-Avian method to navigate images on a worldwide basis was first demonstrated in the North Atlantic Ocean region (Fig. 25). The variability of coastline orientation (islands, lateral distortion, etc.) and

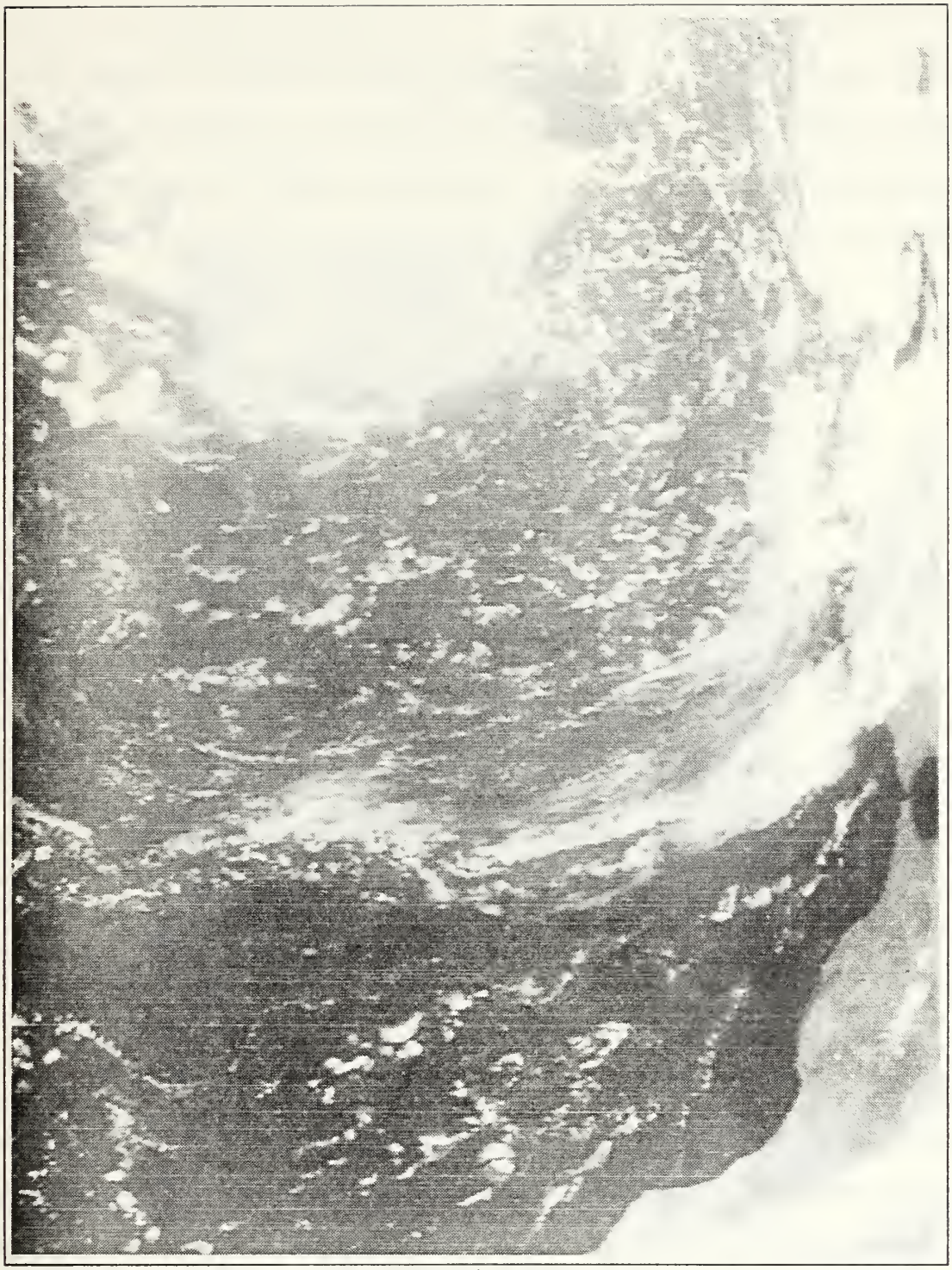

Figure 25 Case 4 AVHRR Overview of NOAA-11 for 155615Z, 8 June, 1992

cloud cover provided multiple opportunities to test the autocorrelation process.

Of particular interest was the performance of the Auto-Avian method on islands and their associated cloud effects. A relatively large island (Maderia) positioned near the satellite's track was selected for testing. The Channel 2

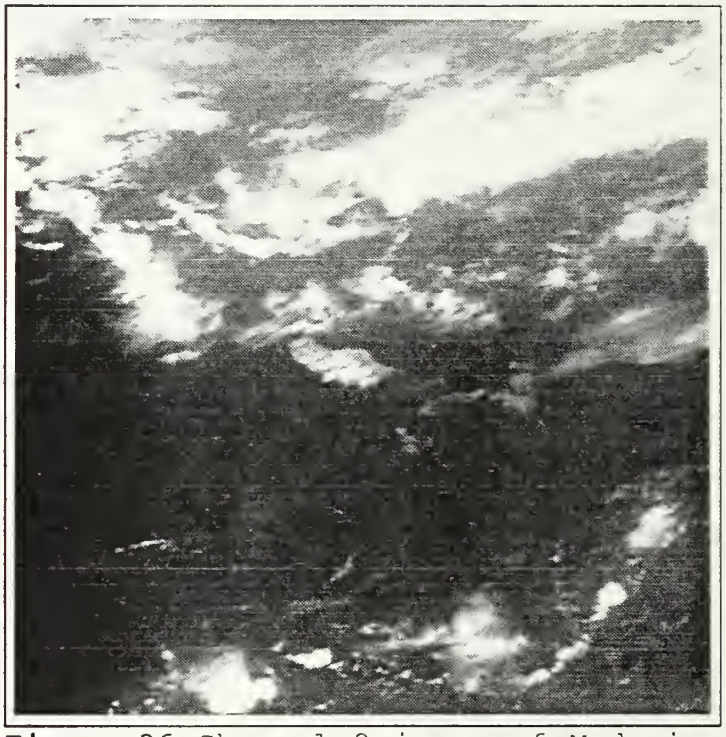

Figure 26 Channel 2 image of Maderia, subscene of Fig 25. The Island is in the center of the image

image of Maderia (Fig. 26) shows a considerable amount of cloud cover on and around the island. In the construction of a binary AVHRR sub-scene, the thresholding and edge enhancement of the Channel 2 image does not reduce the cloud effects, and the cloud edges appear as "false" coastline as

illustrated in Figure 27. Spaulding (1990) noted the adverse effects of this "clutter" on the autocorrelation process. In an attempt to reduce the amount of "clutter", an image utilizing a ratio of albedos (Channel 1/Channel 2) was produced of the same area (Fig. 28). The image provided a

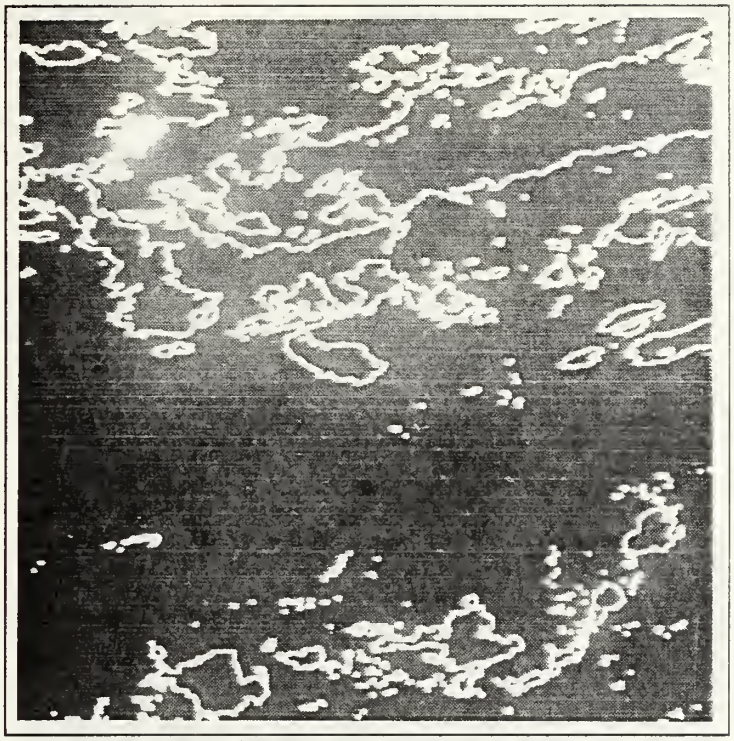

Figure 27 Binary AVHRR (Channel 2) sub-scene (Fig. 26)

distinct contrast between sea, land and clouds that could be subsequently thresholded and edge enhanced to reduce cloud contamination of the binary sub-scene (Fig. 29). It is important to note the large degree of subjectivity involved in the production of the binary AVHRR sub-scene. The threshold values selected for each case were widely varied to reduce cloud effects, yet maintain the integrity of the coastline. The subjective nature of the process may introduce

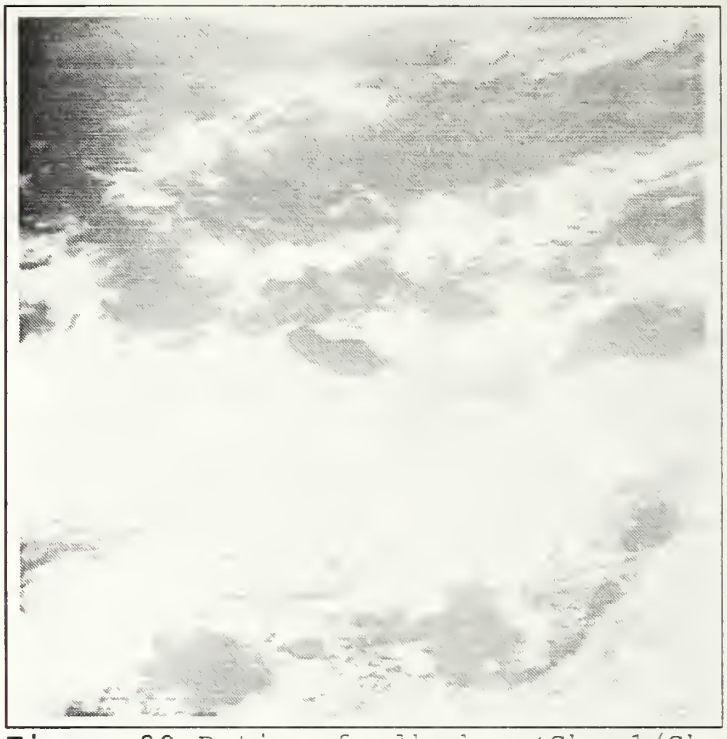

Figure 28 Ratio of albedos (Ch. 1/Ch. 2) image of Maderia.

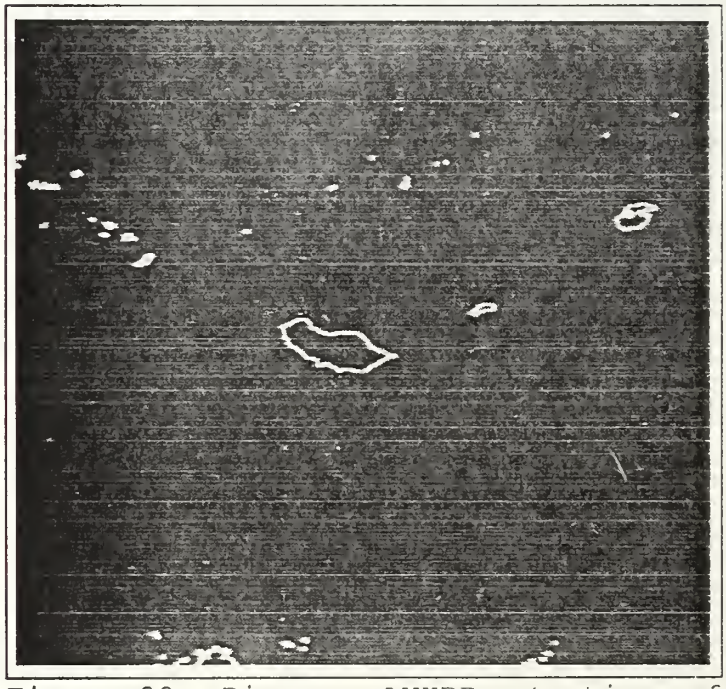

Figure 29 Binary AVHRR (ratio of albedos) sub-scene.

difficulties in further automating the image navigation method.

None the less, the binary AVHRR sub-scene constructed from the albedo ratio image furnished a clear, distinct coastline for cross-correlation. Figure 30 illustrates the results of the Auto-Avian adjustment. Despite the apparent success

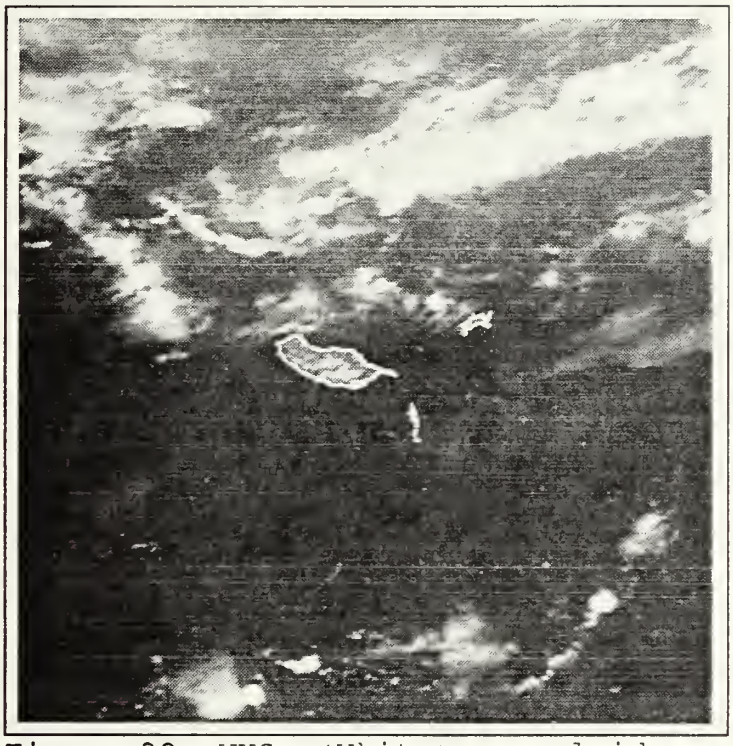

Figure 30 WVS (White) overlaid on image (Channel 2) of Maderia after Auto-Avian adjustment.

of the navigation correction, the residual navigation error (4.29 km) greatly exceeded the average error (1.32 km) obtained by Spaulding (1990) for near nadir locations. Although the spatial resolution of the window area was near optimum (1.1 km), the resolution for the majority of the

control points used to calculate the residual error was significantly degraded. Due to the landmass distribution throughout the orbit, 6 of the 8 control points were located on or near the edges of the image. The subjective error involved in accurately locating these positions within the image most likely affected the residual error calculations. The subjectivety of the process also affected the manual landmarking method resulting in relatively high residual errors (i.e., for the selection of one GCP (7.66 km) and four GCP's (6.12 km) as shown in Table 4).

The Auto-Avian method was also tested on window locations affected by varying degrees of lateral distortion. As previously observed, the residual error increased as the test area was moved from mid-edge (Cape Rhir, MOR) to far-edge (Cape Spartel, MOR). The error ranged from 9.55 km for the mid-edge window to 9.70 km for the far-edge window (Table 4). Figure 31 illustrates the residual navigation error for the far-edge case after the Auto-Avian method had been applied. The spatial resolution of the HRPT imagery for the displaced window location (~775 n mi.) was estimated to be 1.4 n mi. (2.6 km) from Figure 20 (NEPRF, 1983). Accounting for the decrease in resolution, the calculated residual error was approximately 3.7 pixels. Contrary to the calculated value, the slight offset observed in Figure 31 appears to indicate that the subjective error in identifying the control points biased the residual error calculations.

5. Case 5

An image of the Persian Gulf region (Fig. 32) provided the opportunity to test the performance of the Auto-Avian method on a wide range of shoreline geometries. The coastal

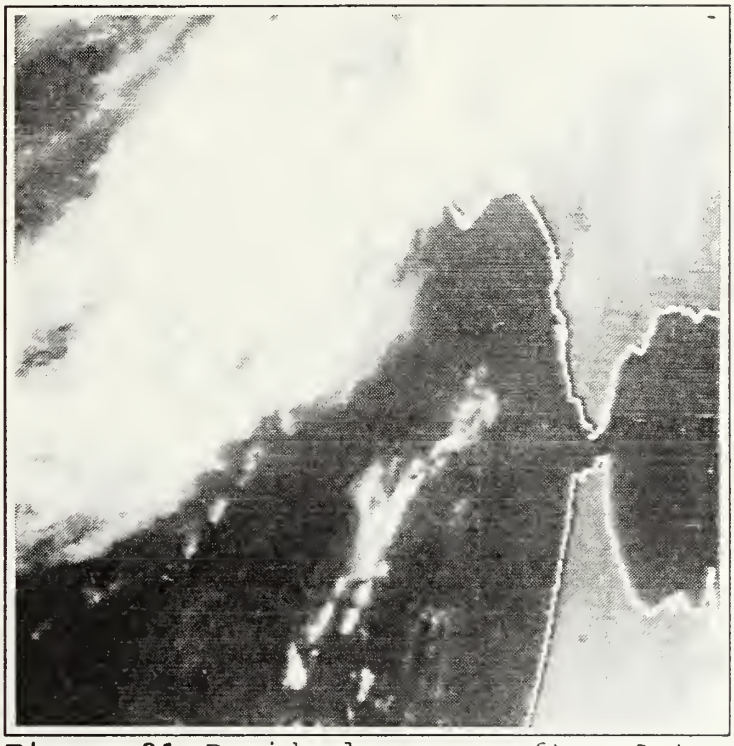

Figure 31 Residual error after Auto-Avian method

features tested included (1) a single small island, (2) simple linear shoreline and (3) an island in close proximity to the shoreline. All of the selected features were located close to the satellite's ground track to minimize distortion. Figure 33 displays the location of each feature before utilizing the Auto-Avian method.

The island of Abu Musa (1) was selected for testing due to its small size (5.4 km) and separation from other coastal

Figure 32 Case 5 AVHRR Overview of NOAA-11 for 102623Z, 1 March, 1991

features. The accuracy of the Auto-Avian method was 1.73 km (Table 4) and compared well to the accuracies obtained by Spaulding (1990). The successful results of the auto-

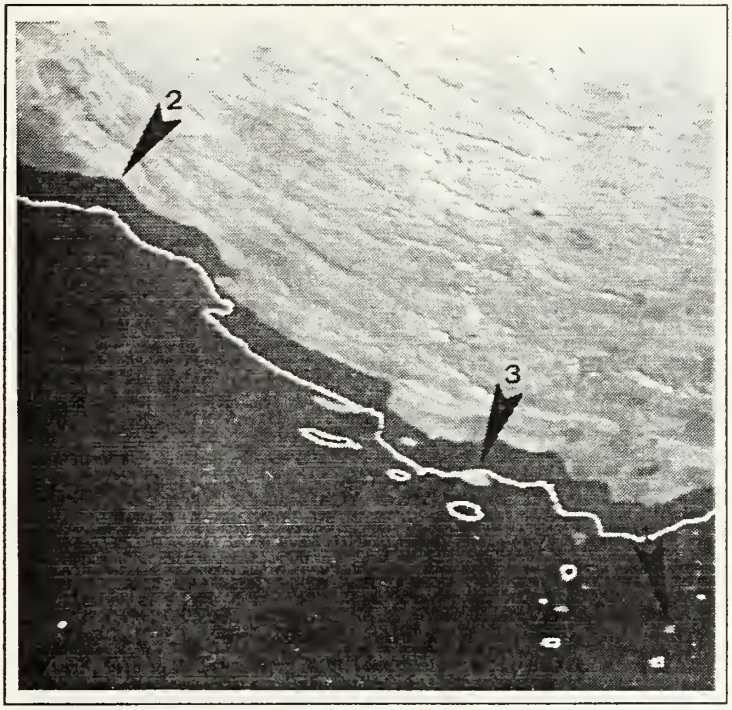

Figure 33 Coastal feature locations before Auto-Avian. (1) Single Island, (2) Simple Coastline and (3) Island-Coast Combination.

correlation process are illustrated in Figure 34.

A rather simple shoreline (2) near Kangān, Iran, was chosen to investigate how coastline "uniqueness" affects the matching process. A rather large error (4.12 km) remained in the image after the application of the Auto-Avian adjustment. The magnitude of this residual error seems to indicate that the selected coastal feature must possess a greater degree of "roughness" to ensure a good match.

Finally, the Auto-Avian method was utilized on a more complex shoreline geometry. An island-coastline combination (3) tested the capabilities of the autocorrelation process to

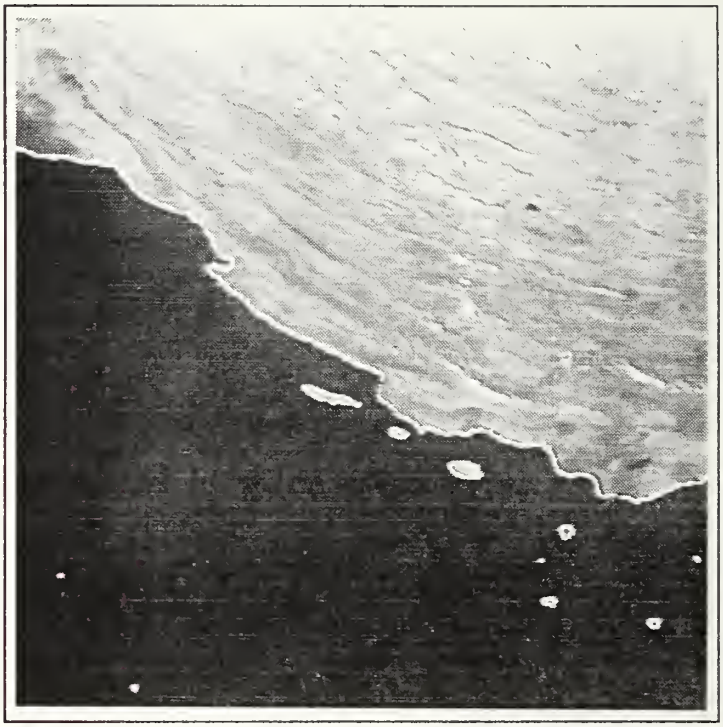

Figure 34 Coastal features after Auto-Avian.

discriminate between two, geometrically similar shorelines. The Auto-Avian method had difficulties correlating the two separate features as illustrated in Figure 35. A comparison of the WVS (white) offset before and after the Auto-Avian adjustment (Figs. 33 and 35 respectively) appears to indicate that the method attempted to match the landmass coastline with the southern shore of the island. The exact cause of the "mismatch" has not been determined and requires further study.

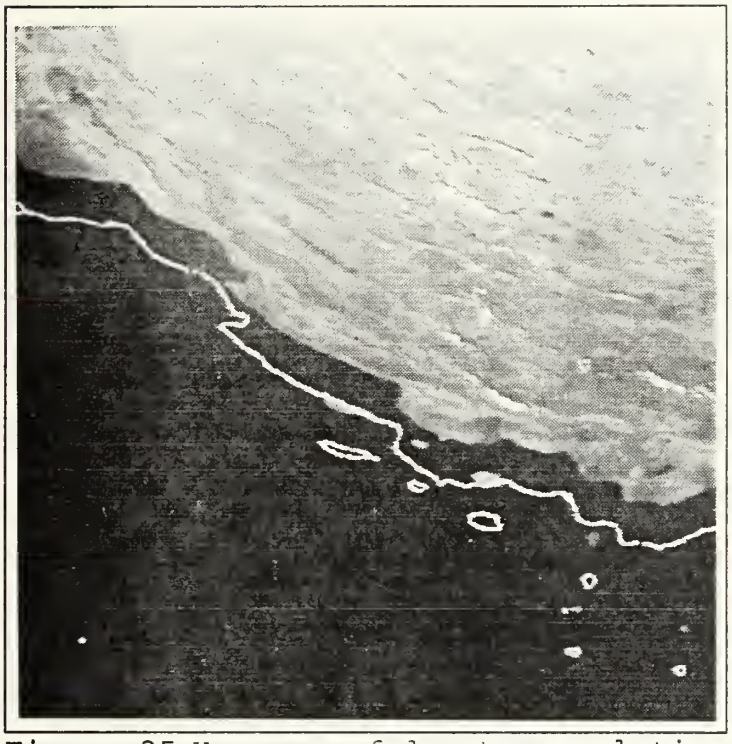

Figure 35 Unsuccessful autocorrelation of island-coastline combination.

V. CONCLUSIONS AND RECOMMENDATIONS

A. CONCLUSIONS

This study successfully demonstrated various aspects of the automated satellite image navigation (Auto-Avian) method developed by Spaulding (1990). The Auto-Avian method replaced the manual procedure of selecting GCP's with an autocorrelation process that utilizes reference shoreline as a "string" of GCP's to rectify satellite images. Spaulding (1990) successfully tested the Auto-Avian method in the eastern North Pacific Ocean region on coastlines located near and along the satellite's track. The automated method achieved near "optimal" (1.1 km) accuracies which were comparable to the manual method with four landmarks (Spaulding, 1990).

The scope of Spaulding's (1990) research was expanded by this study. The worldwide applicability of the Auto-Avian method was successfully demonstrated in three world regions (eastern North Pacific Ocean, eastern North Atlantic Ocean and Persian Gulf). In the process, the capabilities to extract, reduce and display the WVS data from diskette storage were developed and tested. These enhancements in extracting the reference WVS data may facilitate future automation of the extraction process.

The performance of the Auto-Avian method on "less than optimum" images was also investigated by this research. A wide variety of coastline orientations (extreme lateral edge, islands, island-shoreline combination, etc.) with varying degrees of distortion and cloud cover were tested. Accounting for the spatial resolution variations of the window and control point locations (i.e., lateral edge), the accuracies obtained in most cases were comparable to the accuracies reported by Spaulding (1990) for near nadir cases. In the less successful situations (simple coastline and island-shoreline combination), the results of this study indicate that the parameters of shoreline roughness and geometry may play a key role in the autocorrelation process.

Finally, the cloud reduction techniques used by Spaulding (1990) to enhance the land-water interface were studied. The research showed that utilizing a ratio of albedos (Channel 1/Channel 2) significantly reduced cloud effects in the construction of the binary AVHRR sub-scene. The resulting reduction of "clutter" presented a larger amount of "clear" coastline upon which to apply the Auto-Avian method. The technique, however, was quite subjective in nature which may hamper future efforts to automate the process.

B. RECOMMENDATIONS

An automated satellite image navigation system with "optimal" accuracy is rapidly becoming an operational

necessity. The Auto-Avian method is a step in the right direction, but could be improved as follows:

1. Transition To The UNIX System

Currently the Auto-Avian method is performed on a VAX 3000 computer system. The autocorrelation routine (Auto program) alone requires approximately 12½ minutes of CPU time. Due to the limited capability of the VAX system (~3 MIPS), the actual run time of the program takes hours. Transitioning the Auto-Avian method to the UNIX system (~20-30 MIPS) should significantly reduce run time and thereby facilitate utilization on an operational basis.

2. Increase The Level of Automation

As described in Chapter II, the Auto-Avian method requires the use of three separate routines (Extraction, Binary and Auto). At the very least, the routines could be linked together to reduce the time required to utilize the method. The ideal situation would incorporate a cloud detection algorithm similar to the one used by Bordes et al. (1991) to automatically identify relatively cloud free coastline for cross-correlation with the WVS. The modification would definitely decrease the amount of operator interaction and may subsequently reduce the processing time.

3. Start Operational Use and Testing

Up to this point, the Auto-Avian method has been utilized on an experimental basis only. The results of this

study have shown that the automated method can navigate a wide variety of images as accurately as manual landmarking procedures. Based on this validation, the Auto-Avian method should become operational to gather operator feedback and statistical data on the accuracy of the method. Auto-Avian should be used on the daily passes received at NPS with its new HRPT capability. These types of studies will lead to better navigation for future operational military satellite display systems such as the Tactical Environmental Support System 3 (TESS 3).

LIST OF REFERENCES

Anuta, P. and C. McGillem, 1986: Parameter space techniques for image registration. IGARSS '86. *Remote Sensing: Today's Solutions for Tomorrow's Information Needs,* August 1986 (ESA SP-254), **2**, 989-994.

Bethke, W.J., 1988: Accuracy of satellite data navigation. *M.S. Thesis, Naval Postgraduate School,* Monterey, CA, 87 pages

Bowditch, Nathaniel, 1984 ed. American practical navigator: an epitome of navigation. Defense Mapping Agency Hydrographic/Topographic Center, Washington, D.C.

Bordes, Philippe, Pascal Brunel and Anne Marsouin, 1991: Automatic adjustment of AVHRR navigation. *Journal of Atmospheric and Oceanic Technology,* **9**, 15-27.

Brunel, P. and A. Marsouin, 1987: Geographic navigation of NOAA AVHRR series imagery. *SATMOS Notes No 2-CMS B.P. 147 22303 Lannion France,* 1-81.

Brush, R.J.H., 1988: The navigation of AVHRR imagery. *International Journal of Remote Sensing,* **9**, 1491-1502.

Cordan, Earnest W., Jr. and Benjamin W. Patz, 1979: An image registration algorithm using sampled binary correlation. *1979 Machine Processing of Remotely Sensed Data Symposium, IEEE,* 202-211.

Crombie, M.A., 1983: Coordination of stereo image registration and pixel classification. *Photogrammetric Engineering and Remote Sensing,* **49**, 529-532.

Defense Mapping Agency, 1988: Product specifications for world vector shoreline. DMA Hydrographic/Topographic Center, Washington D.C.

Defense Mapping Agency, 1990: Datums, ellipsoids, grids and grid reference systems. *DMA Technical Manual 8358.1,* DMA Hydrographic/Topographic Center, Washington D.C.

Douglas, David H. and Thomas K. Peuker, 1973: Algorithms for the reduction of the number of points required to represent a digitized line or characterture. *Canadian Cartographer,* **10**, 112-122.

Emery, William J., J. Brown and Z. P. Nowak, 1989: AVHRR image navigation: summary and review. *Photogrammetric Engineering and Remote Sensing,* **55**, 1175-1183.

Emery, W. J. and M. Ikeda, 1984: A comparison of geometric correction methods for AVHRR imager. *Canadian Journal of Remote Sensing,* **10**, 46-56.

Eversole, William L. and Robert E. Nasburg, 1983: Maximum likelihood estimation for image registration. *Applications of Digital Image Processing VI, Proceedings of SPIE-The International Society of Optical Engineers,* **432**, 190-194.

Goshtasby, A., S. H. Gage and J. F. Bartholic, 1984: A two-stage cross correlation approach to template matching. *IEEE Transactions on Pattern Analysis and Machine Intelligence,* **PAMI-6**, 374-378.

Goshtasby, A., G. C. Stockman and C. V. Page, 1986: A region-based approach to digital image registration with subpixel accuracy. *IEEE Transactions on Geoscience and Remote Sensing,* **GE-24**, 390-399.

Hall, Ernest L., 1979: Computer image processing of remotely sensed data. Academic Press, Inc. New York, 256 pages.

Hendersen, T.C., E. E. Triendl and R. Winter, 1985: Edge- and shape-based geometric registration. *IEEE Transactions on Geoscience and Remote Sensing,* **GE-23**, 334-342.

Ho, Diem and A. Asem, 1986: NOAA AVHRR image referencing. *International Journal of Remote Sensing,* **7**, 895-904.

Hord, Michael R., 1982: Digital Image processing of remotely sensed data. Academic Press, Inc., New York, 256 pages.

Jayroe, R. R., J. F. Andrus and S. W. Campbell, 1974: Digital image registration method based upon binary boundary maps. *National Aeronautics and Space Administration,* NASA-TN-D-7607: m-**121**.

Jullien, J.P. and T. Phulpin, 1988: Automatic adjustment of the AVHRR navigation. *Note de Travail de L'EERM, METEOFRANCE,* 1-30.

Kloster, K., 1989: Using TBUS orbital elements for AVHRR image gridding. *International Journal of Remote Sensing,* **10**, 653-659.

Moik, Johannes G., 1980: Digital processing of remotely sensed data. National Aeronautics and space Administration, NASA SP; 431 pages.

Nack, M. L., 1977: Rectification and registration of digital images and the effect of cloud detection. *4th Annual Symposium on Machine Processing of Remotely Sensed Data 21-23 June 1977,* West Lafayette, Indiana, 12-23.

Navy Environmental Prediction Research Facility, 1983: Navy tactical applications guide: operational environmental satellites. *NEPRF Technical Report TR83-02,* Tactical Applications Department, Monterey, CA.

Saunders, R. W. and K. T. Kriebal, 1988: An improved method for detecting clear sky and cloudy radiances from AVHRR data. *International Journal of Remote Sensing,* **9**, 123-150.

Spaulding, Brian C., 1990: Automatic satellite image navigation. M. S. Thesis, Naval Postgraduate School, Monterey, CA, 83 pages.

Vanderbrug, Gordan J. and Azriel Rosenfeld, 1977: Two-stage template matching. *IEEE Transactions on Computers,* **C-26**, 384-393.

Wong, Robert Y. and Ernest L. Hall, 1979: Performance comparison of scene matching techniques. *IEEE Transactions on Pattern Analysis and Machine Intelligence,* **PAMI-1**, 325-330.

INITIAL DISTRIBUTION LIST

		No.Copies
1.	Defense Techinical Information Center Cameron Station Alexandria, VA 22304-6145	2
2.	Library, Code 52 Naval Postgraduate School Monterey, CA 93943-5002	2
3.	C.H. Wash (Code MR/WX) Department of Meteorology Naval Postgraduate School Monterey, CA 93943-5000	3
4.	P. Durkee (Code MR/DE) Department of Meteorology Naval Postgraduate School Monterey, CA 93943-5000	1
5.	Chairman (Code MR/HY) Department of Meteorology Naval Postgraduate School Monterey, CA 93943-5000	1
6.	Chairman (Code OC/CO) Department of Oceanography Naval Postgraduate School Monterey, CA 93943-5000	1
7.	Tom Lee Naval Research Laboratory Monterey, CA 93943-5006	1
8.	N.T. Garfield (Code OC/GF) Department of Oceanography Naval Postgraduate School Monterey, CA 93943-5000	1
10.	LCDR Robert M. Bassett Naval Oceanography Command Facility Naval Air Station, North Island P.O. Box 357076 San Diego, CA 92135-7076	1

11. Mike Thomas SC/EGED 1
Stop B-54
Defense Mapping Agency
8613 Lee Hwy
Fairfax, VA 22031-2138

12. Dr. Chris Crosiar 1
Navy Oceanographic and Atmospheric Research Lab
Monterey, CA 93943-5005

194-403

DEMCO

AMERICAN BINDERY
10
9-93

DUDLEY KNOX LIBRARY
3 2768 00032215 0